A theoretical investigation of 38-atom CuPd clusters: the effect of potential parameterisation on structure and segregation - Supplementary Information

Caitlin A. Casey-Stevens, Mingrui Yang, Geoffrey R. Weal,
Samantha M. McIntyre, Brianna K. Nally, and Anna L. Garden

1 Radial distribution functions of all GM clusters from GPSs C, M and P/N, and DFT refinement, for all bimetallic compositions (Cu_1Pd_{37} to $Cu_{37}Pd_1$)
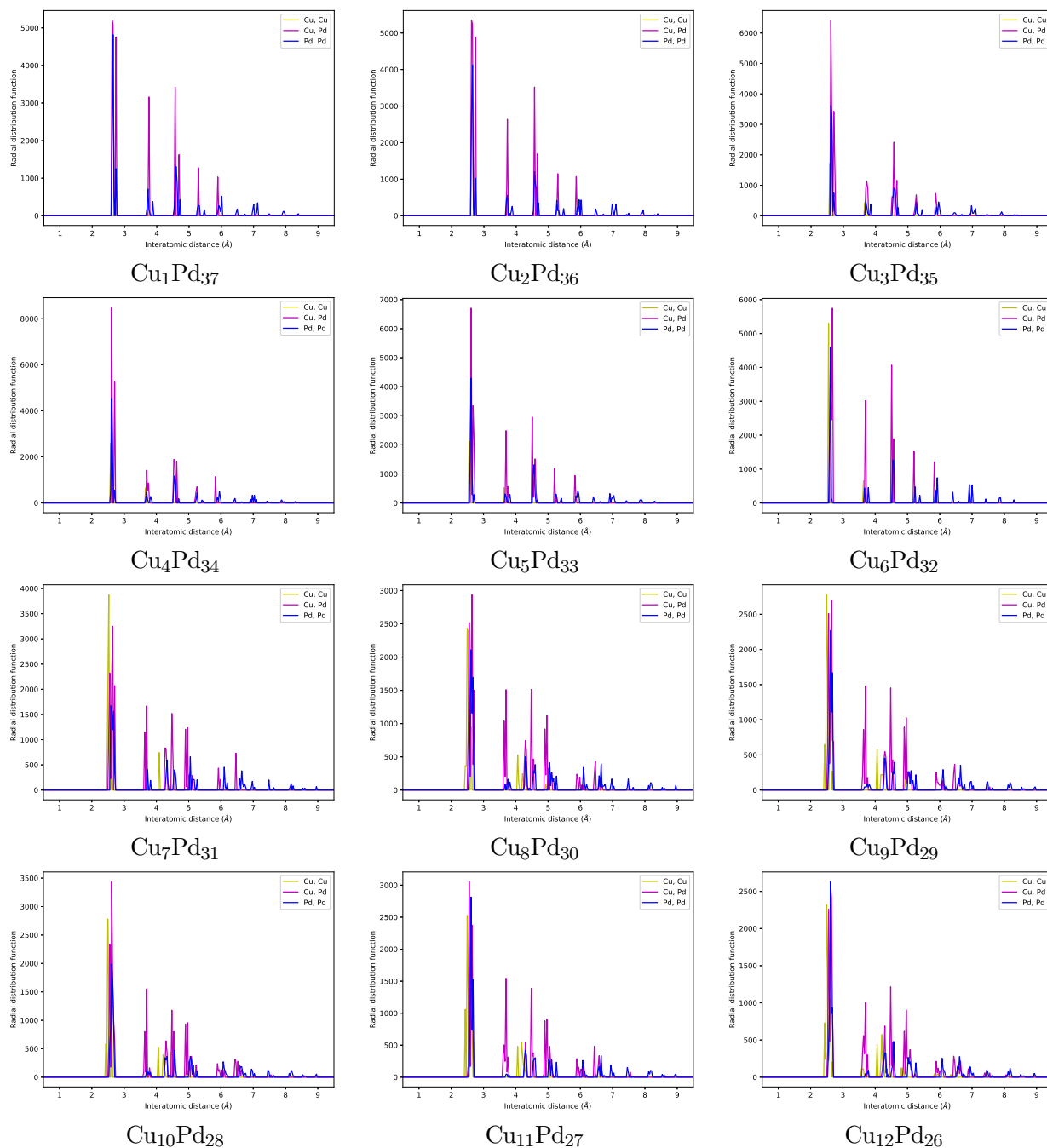

Figure 1: The radial distribution functions calculated for GM clusters of all compositions found in a global optimisation run with GPS C.
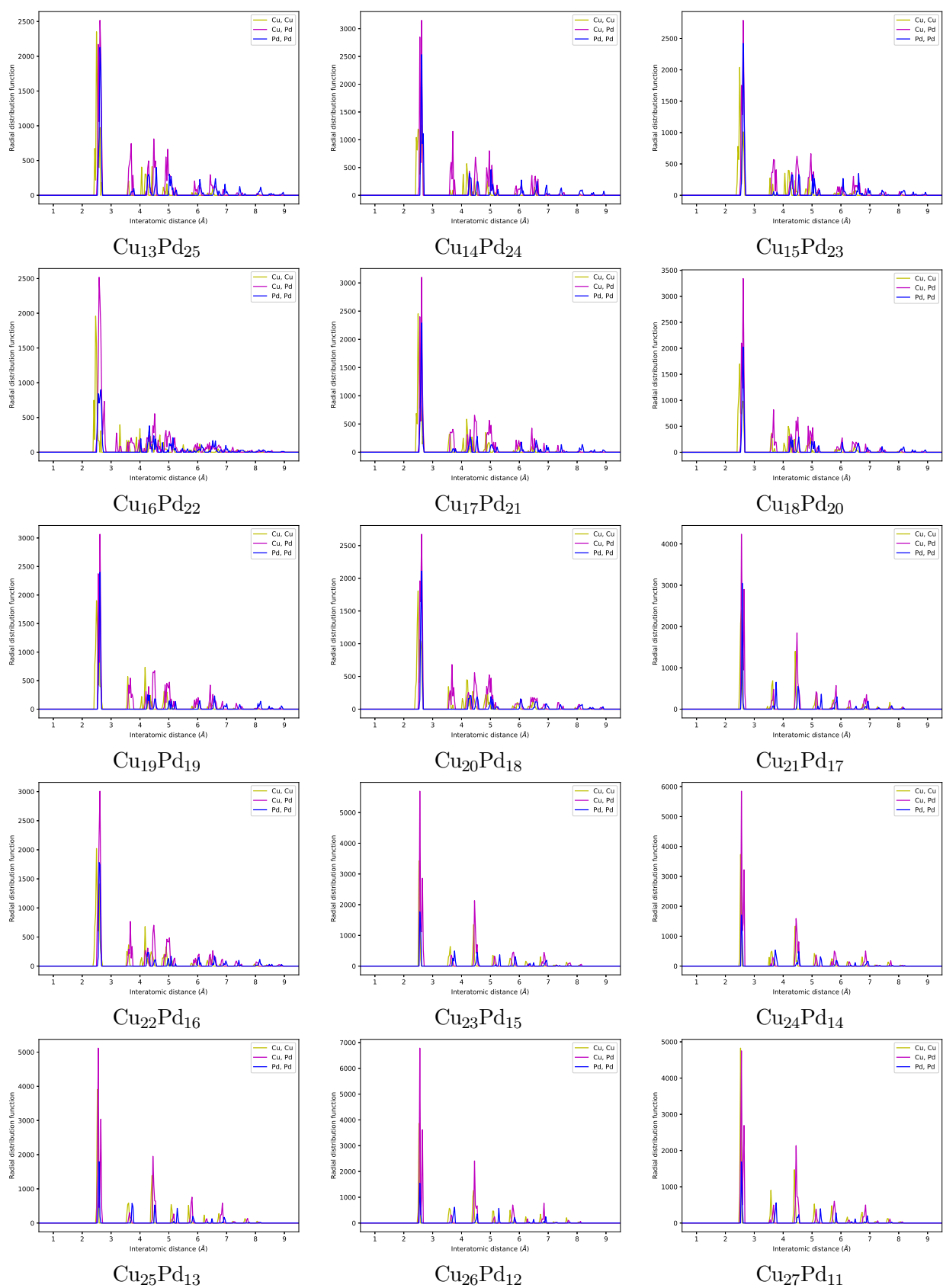
Figure 2: The radial distribution functions calculated for GM clusters of all compositions found in a global optimisation run with GPS C *cont'd*.
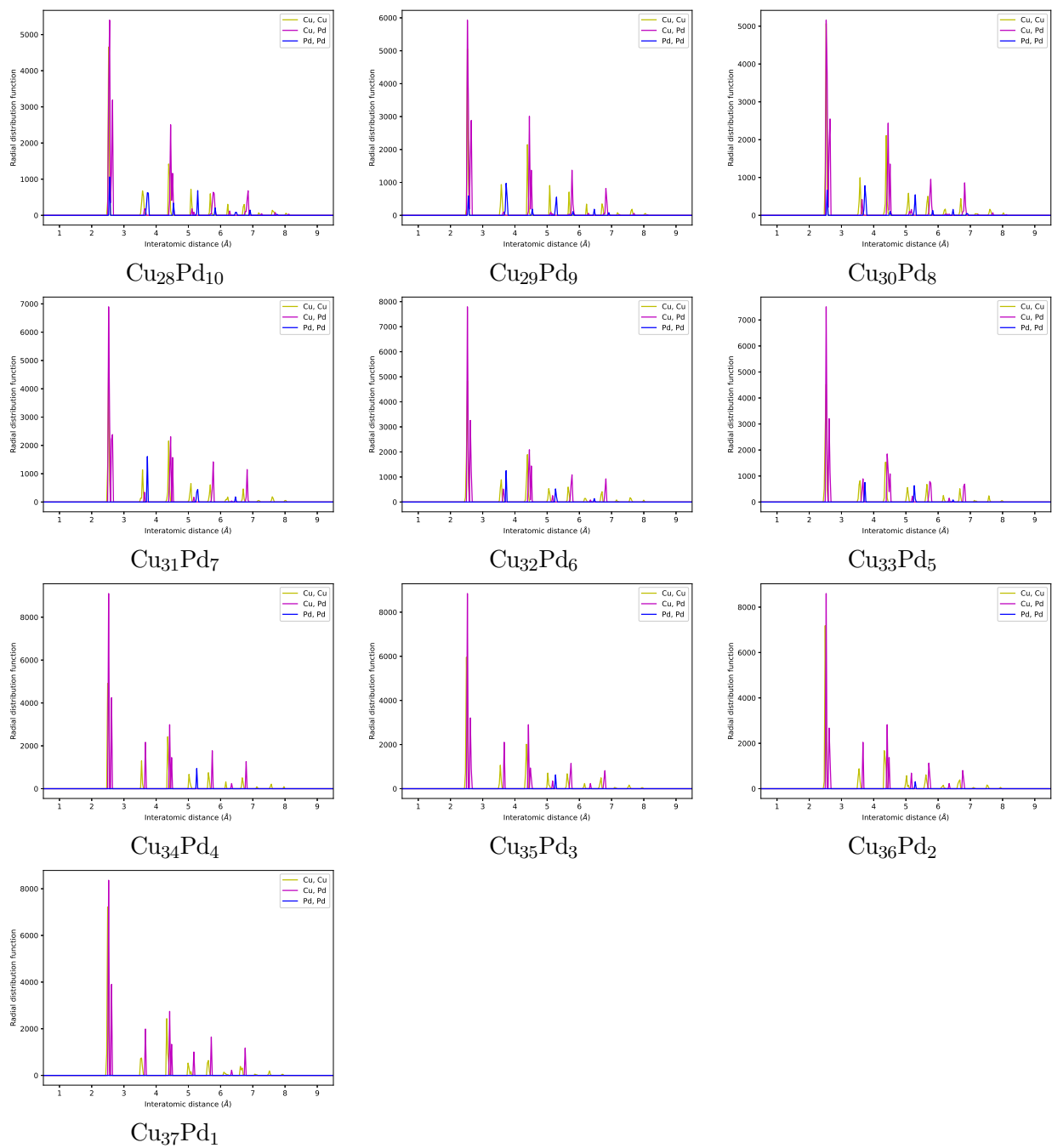
Figure 3: The radial distribution functions calculated for GM clusters of all compositions found in a global optimisation run with GPS C *cont'd.*
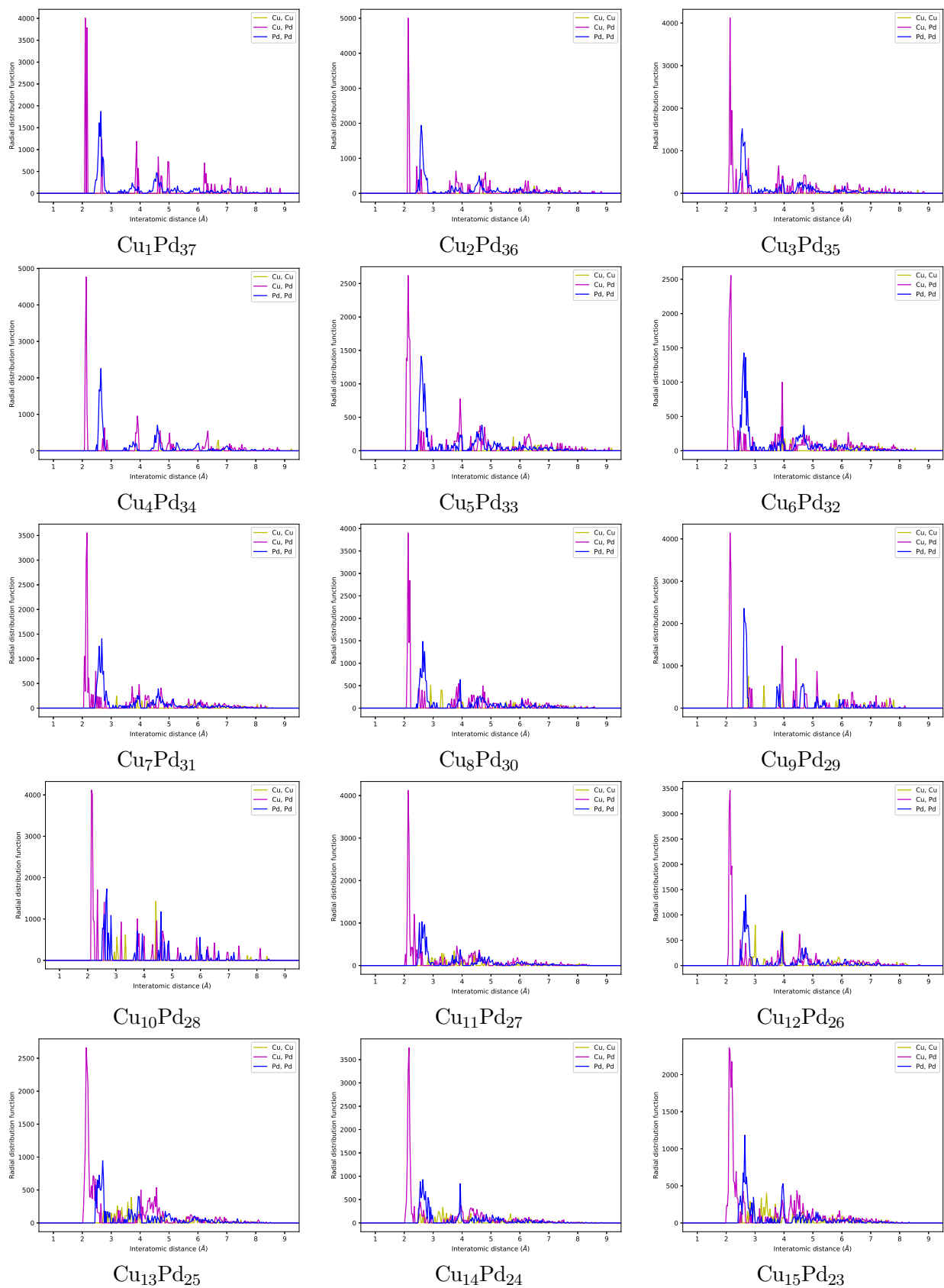
Figure 4: The radial distribution functions calculated for GM clusters of all compositions found in a global optimisation run with GPS M.
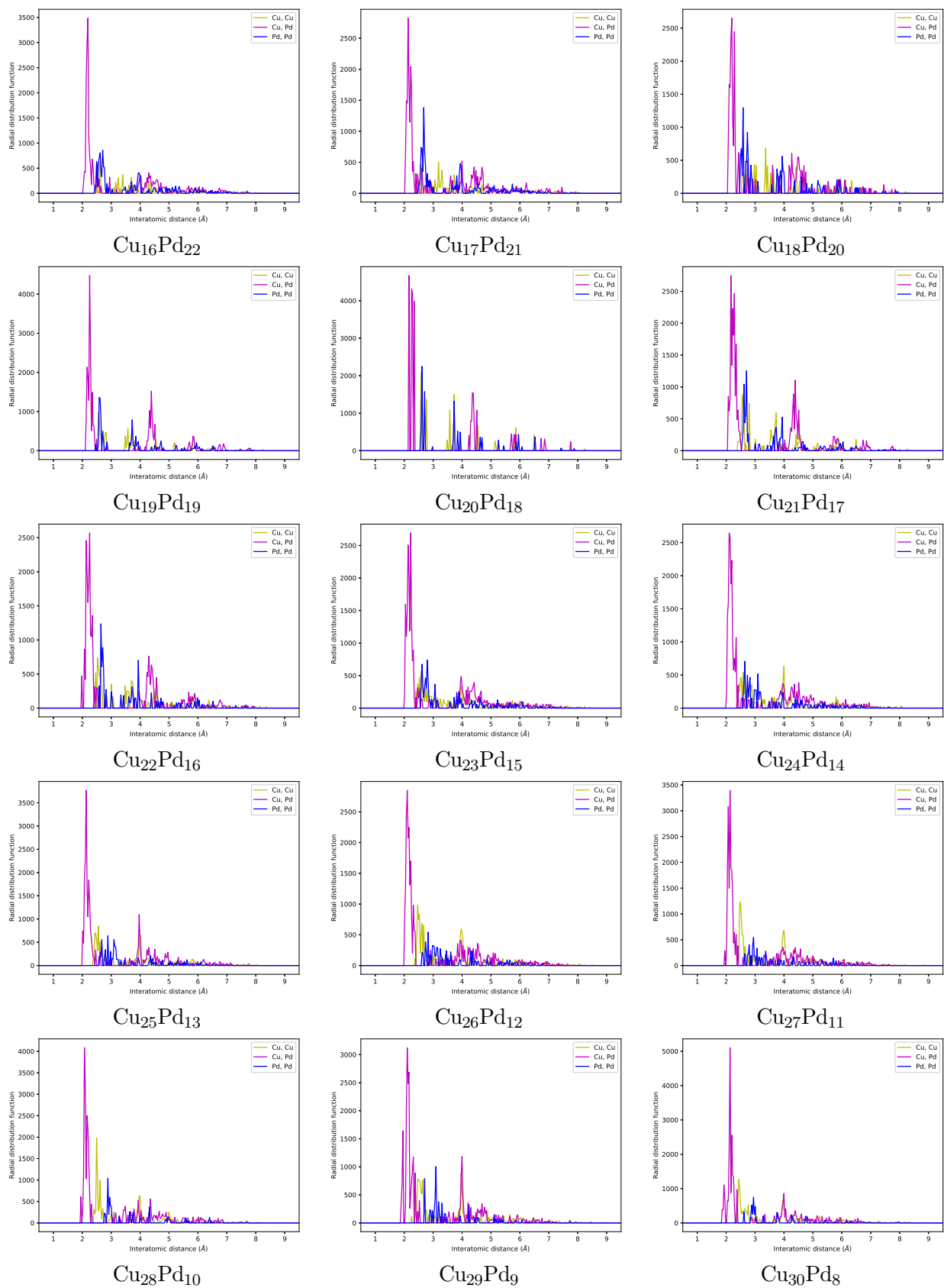
Figure 5: The radial distribution functions calculated for GM clusters of all compositions found in a global optimisation run with GPS M *cont'd.*
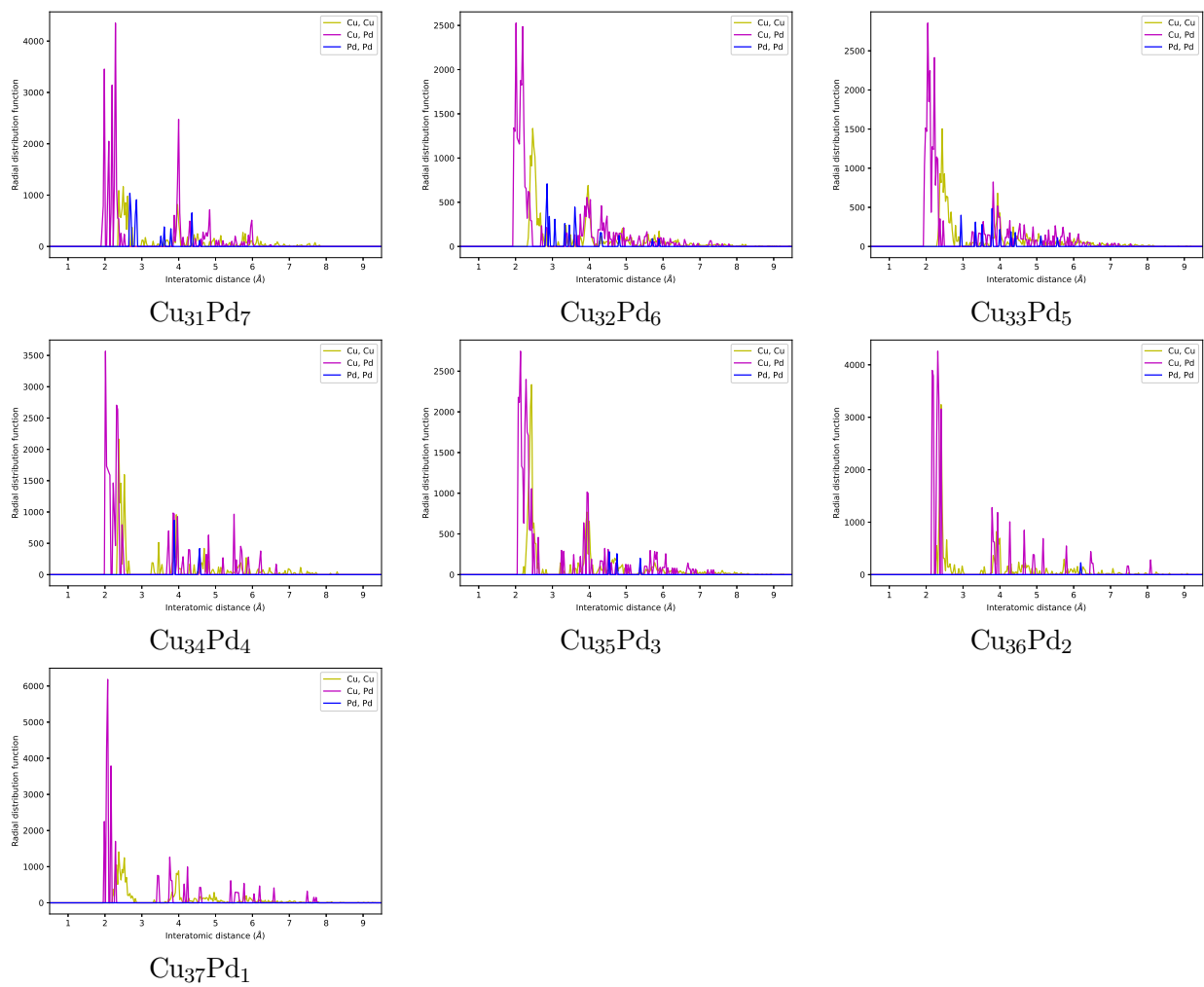
Figure 6: The radial distribution functions calculated for GM clusters of all compositions found in a global optimisation run with GPS M *cont'd.*
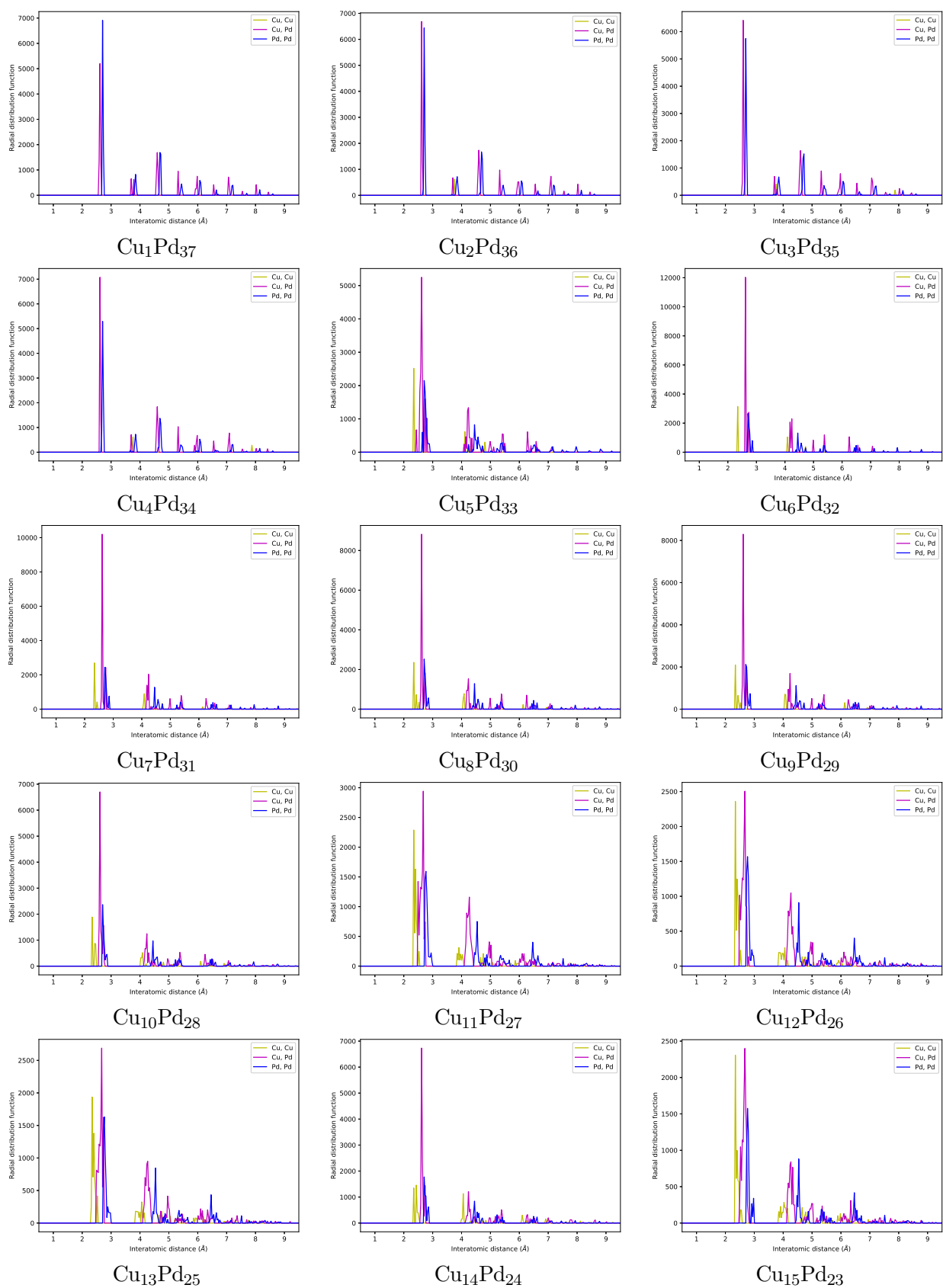
Figure 7: The radial distribution functions calculated for GM clusters of all compositions found in a global optimisation run with GPS P/N.
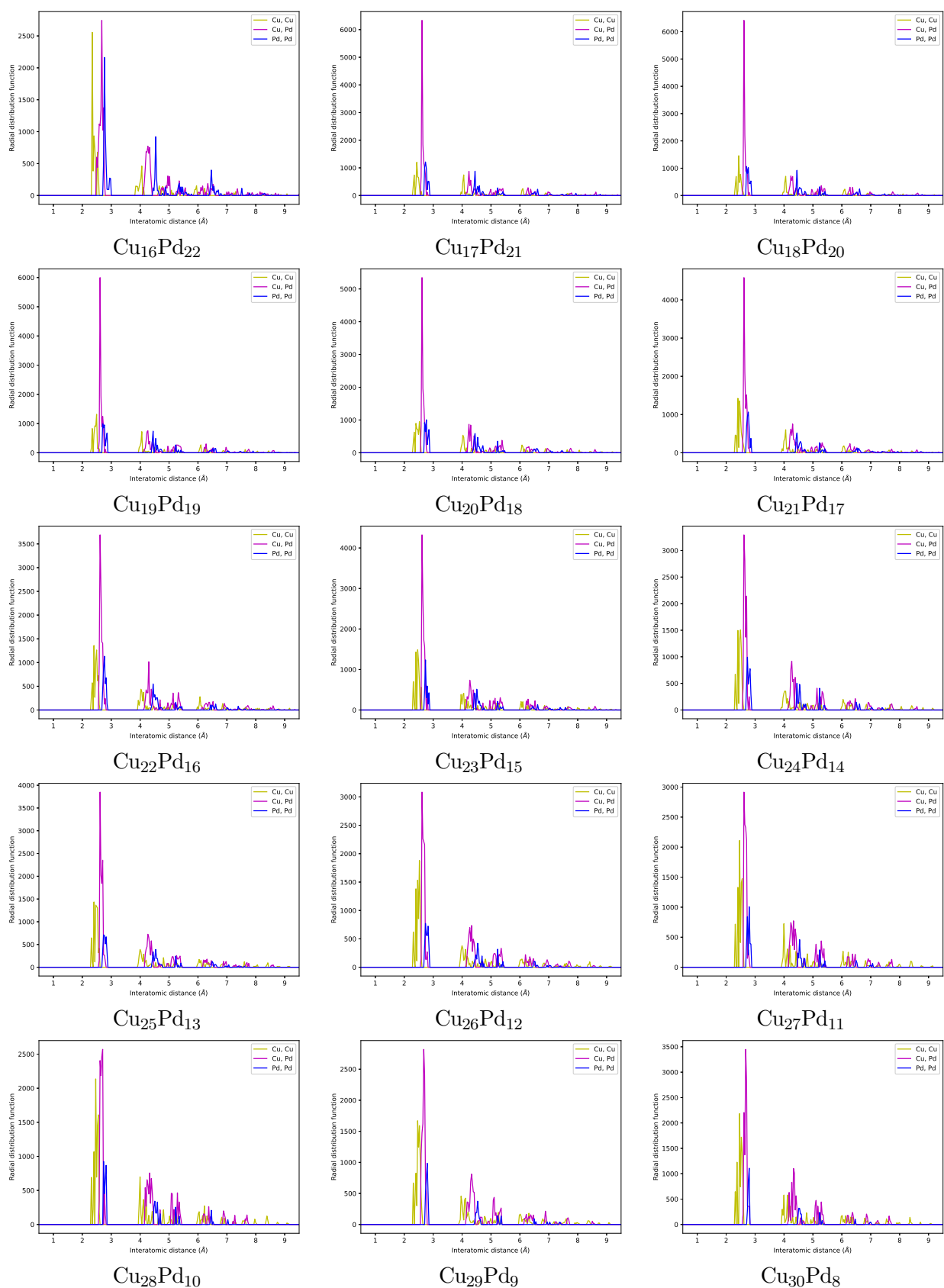
Figure 8: The radial distribution functions calculated for GM clusters of all compositions found in a global optimisation run with GPS P/N *cont'd.*
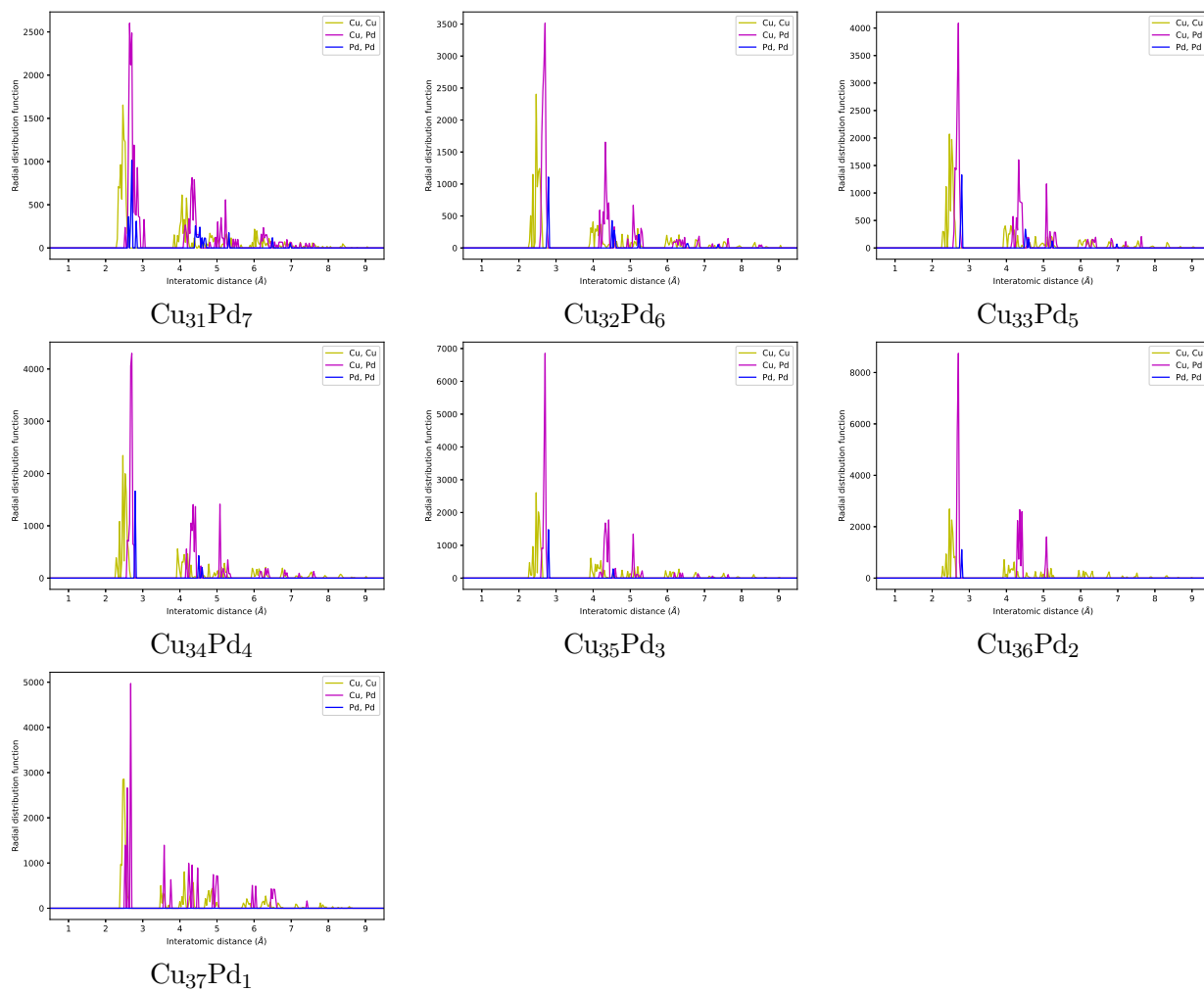
Figure 9: The radial distribution functions calculated for GM clusters of all compositions found in a global optimisation run with GPS P/N *cont'd*.
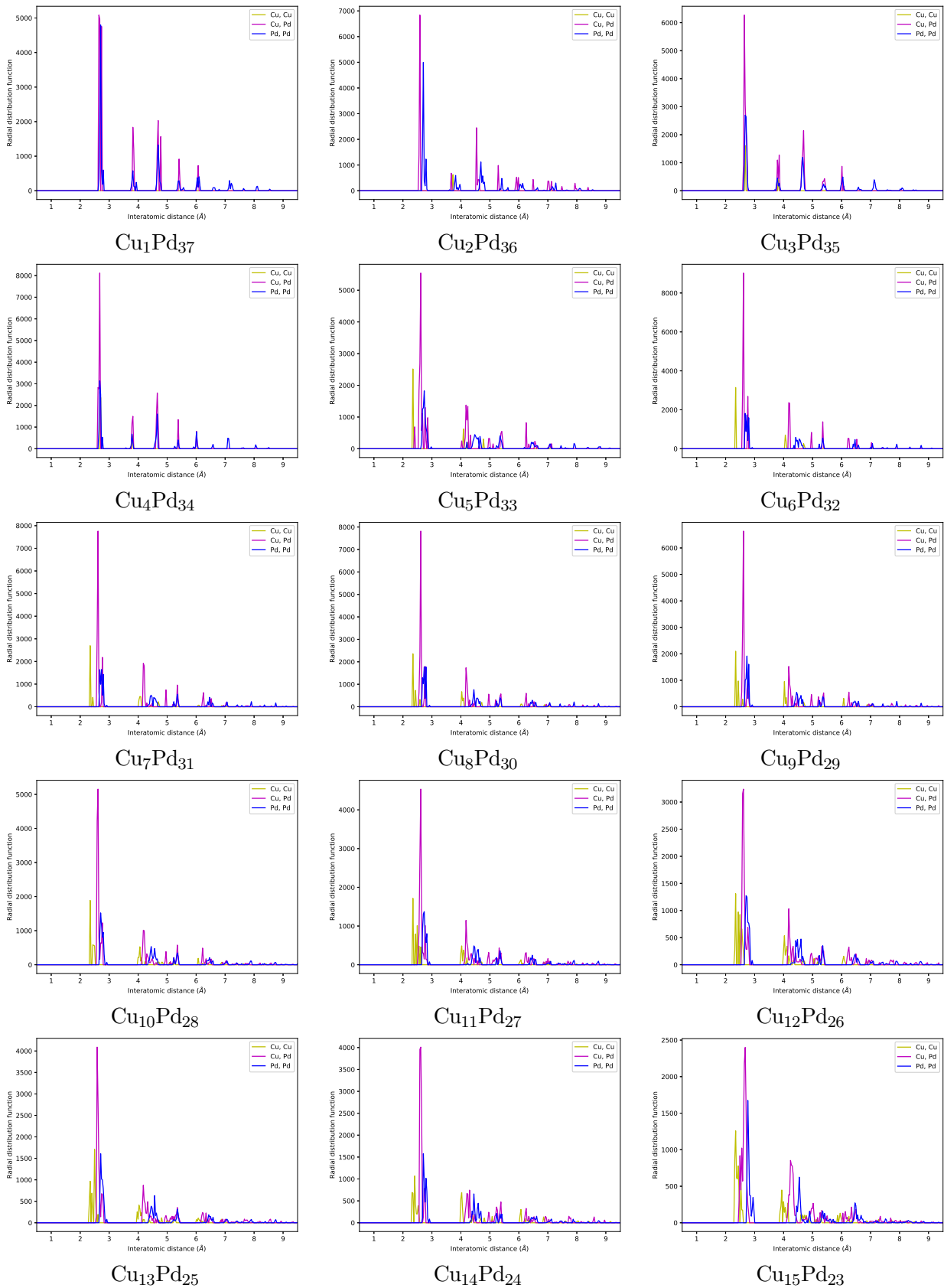
Figure 10: The radial distribution functions calculated for GM clusters of all compositions as found by DFT refinement of the GM clusters from the global optimisation runs of each GPS.

Figure 11: The radial distribution functions calculated for GM clusters of all compositions as found by DFT refinement of the GM clusters from the global optimisation runs of each GPS *cont'd*.

Cu$_{31}$Pd$_7$

Cu$_{32}$Pd$_6$

Cu$_{33}$Pd$_5$

Cu$_{34}$Pd$_4$

Cu$_{35}$Pd$_3$

Cu$_{36}$Pd$_2$

Cu$_{37}$Pd$_1$

Figure 12: The radial distribution functions calculated for GM clusters of all compositions as found by DFT refinement of the GM clusters from the global optimisation runs of each GPS *cont'd*.
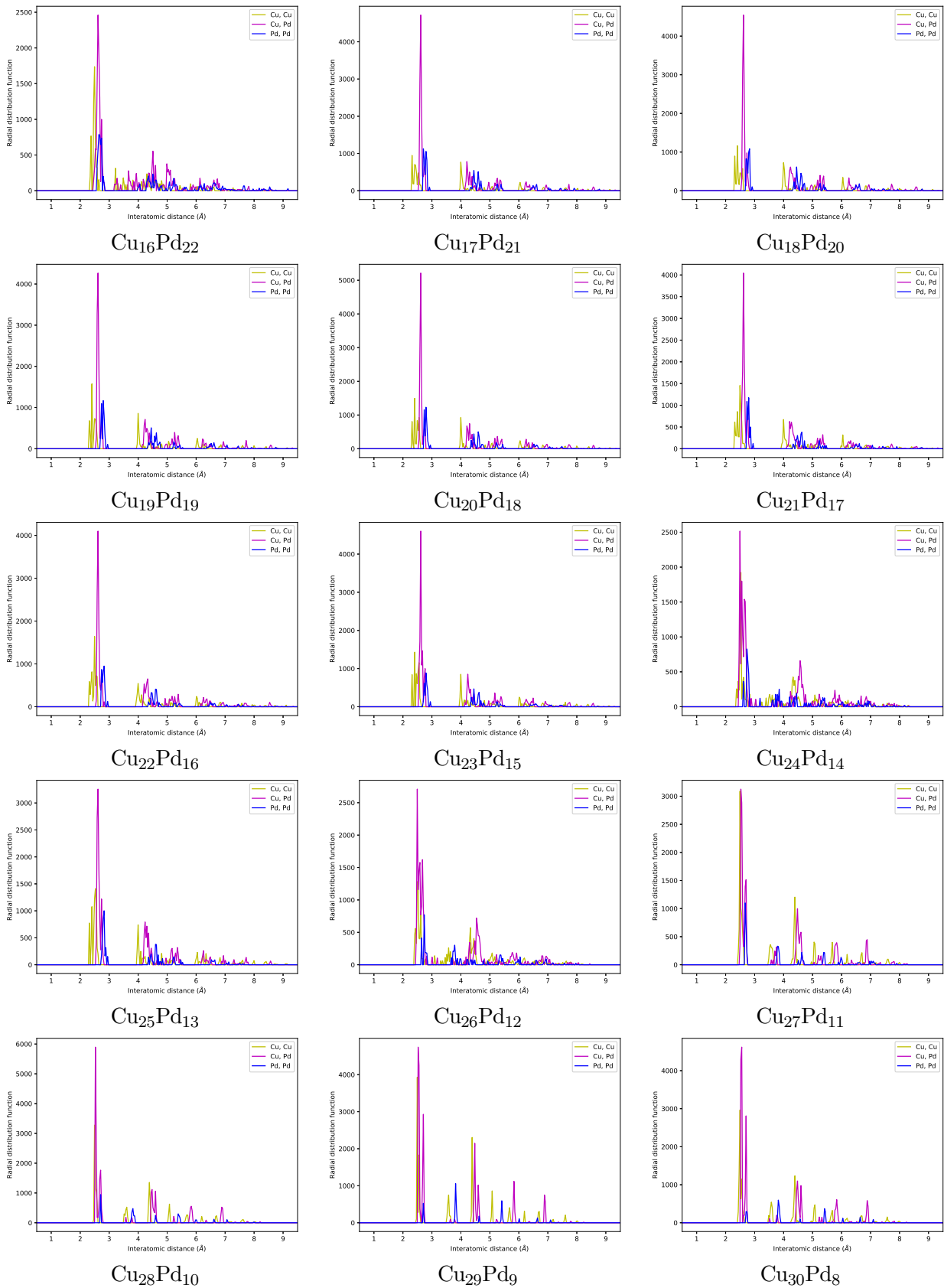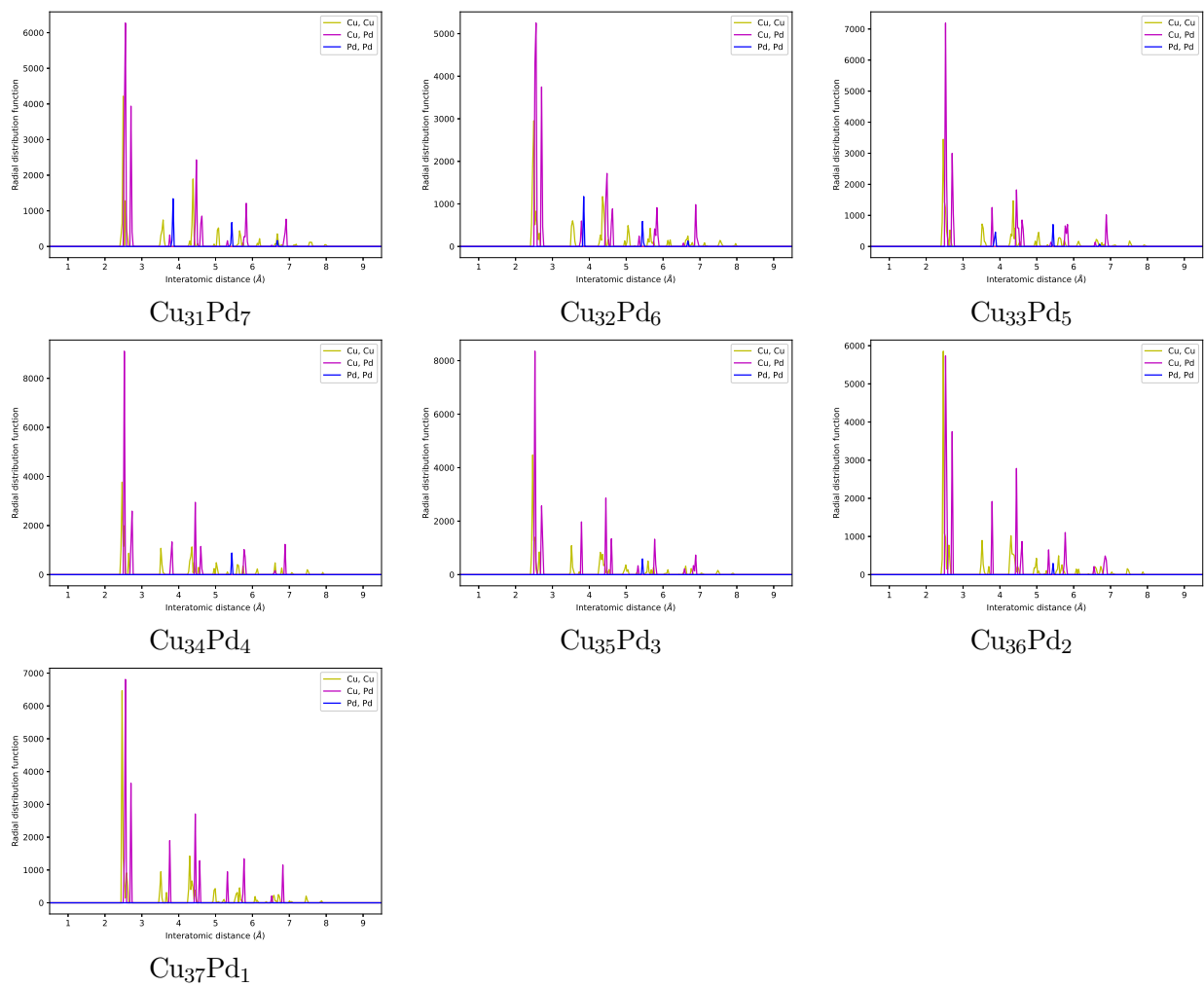
2 Nearest neighbour analyses of all GM clusters from GPSs C, M and P/N, and DFT refinement, for all bimetallic compositions (Cu$_1$Pd$_{37}$ to Cu$_{37}$Pd$_1$)
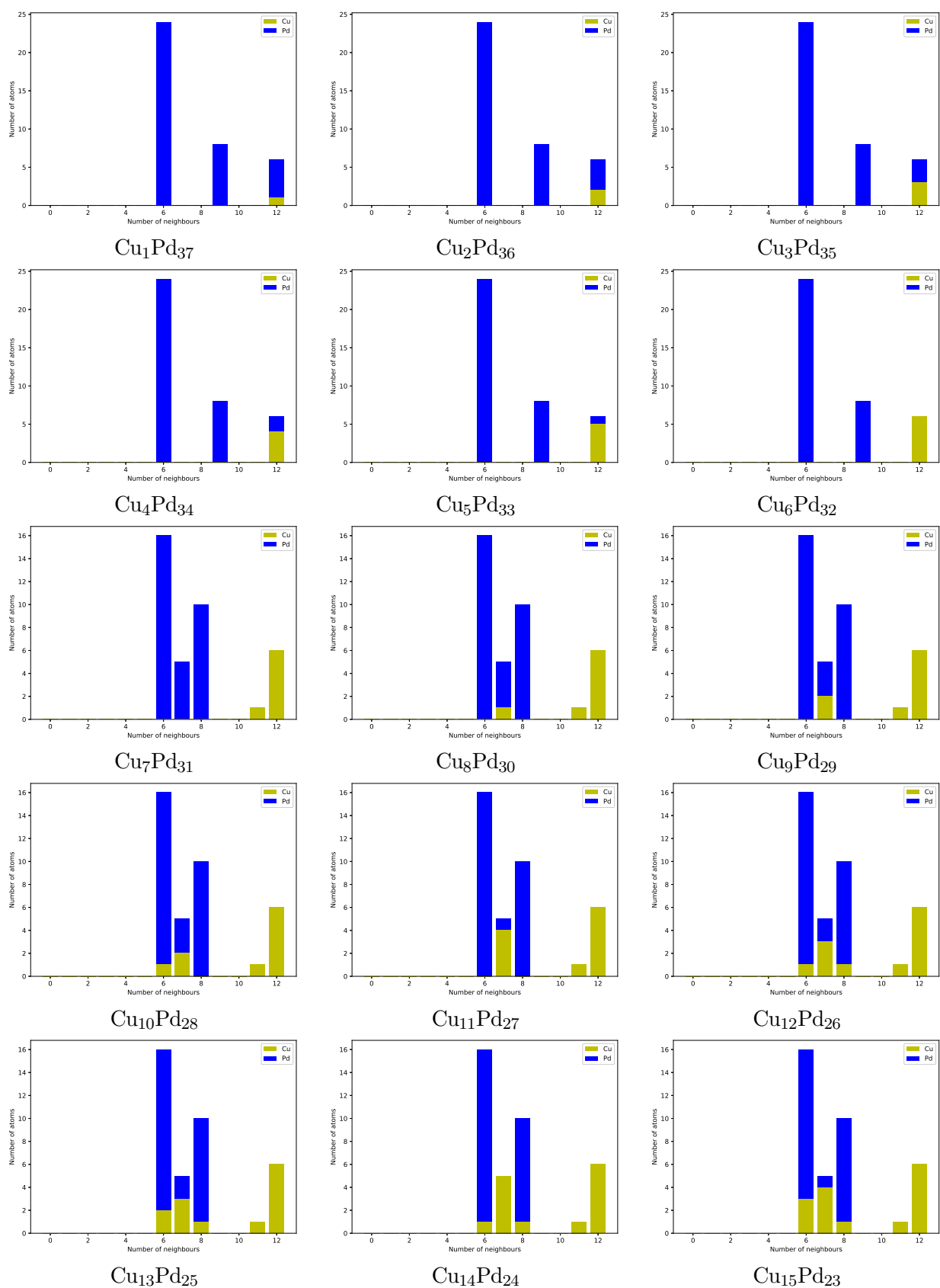

Figure 13: The nearest neighbour analyses calculated for GM clusters of all compositions found in a global optimisation run with GPS C.

Figure 14: The nearest neighbour analyses calculated for GM clusters of all compositions found in a global optimisation run with GPS C *cont'd*.

Cu₃₁Pd₇   Cu₃₂Pd₆   Cu₃₃Pd₅

Cu₃₄Pd₄   Cu₃₅Pd₃   Cu₃₆Pd₂
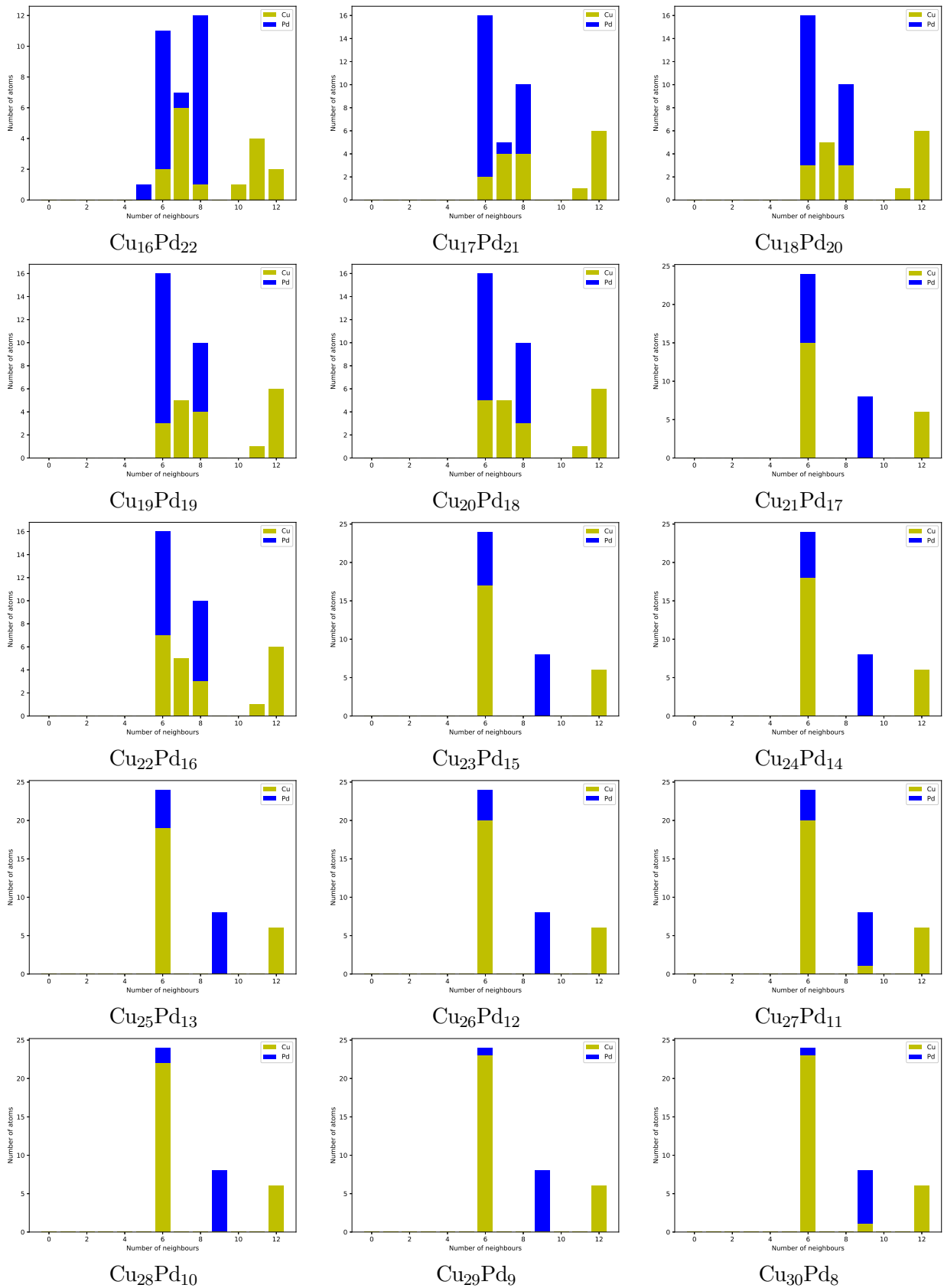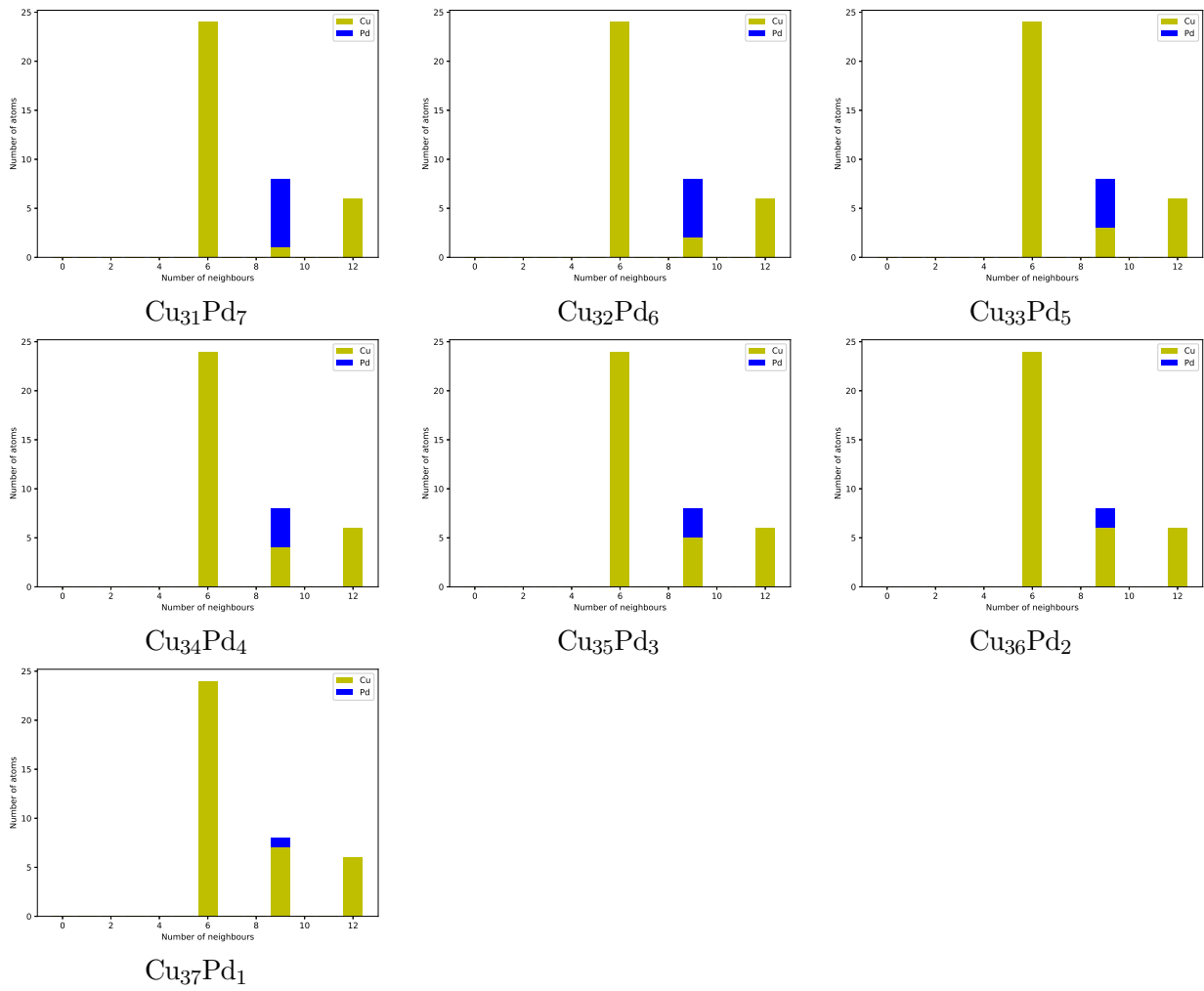
Cu₃₇Pd₁

Figure 15: The nearest neighbour analyses calculated for GM clusters of all compositions found in a global optimisation run with GPS C *cont'd.*
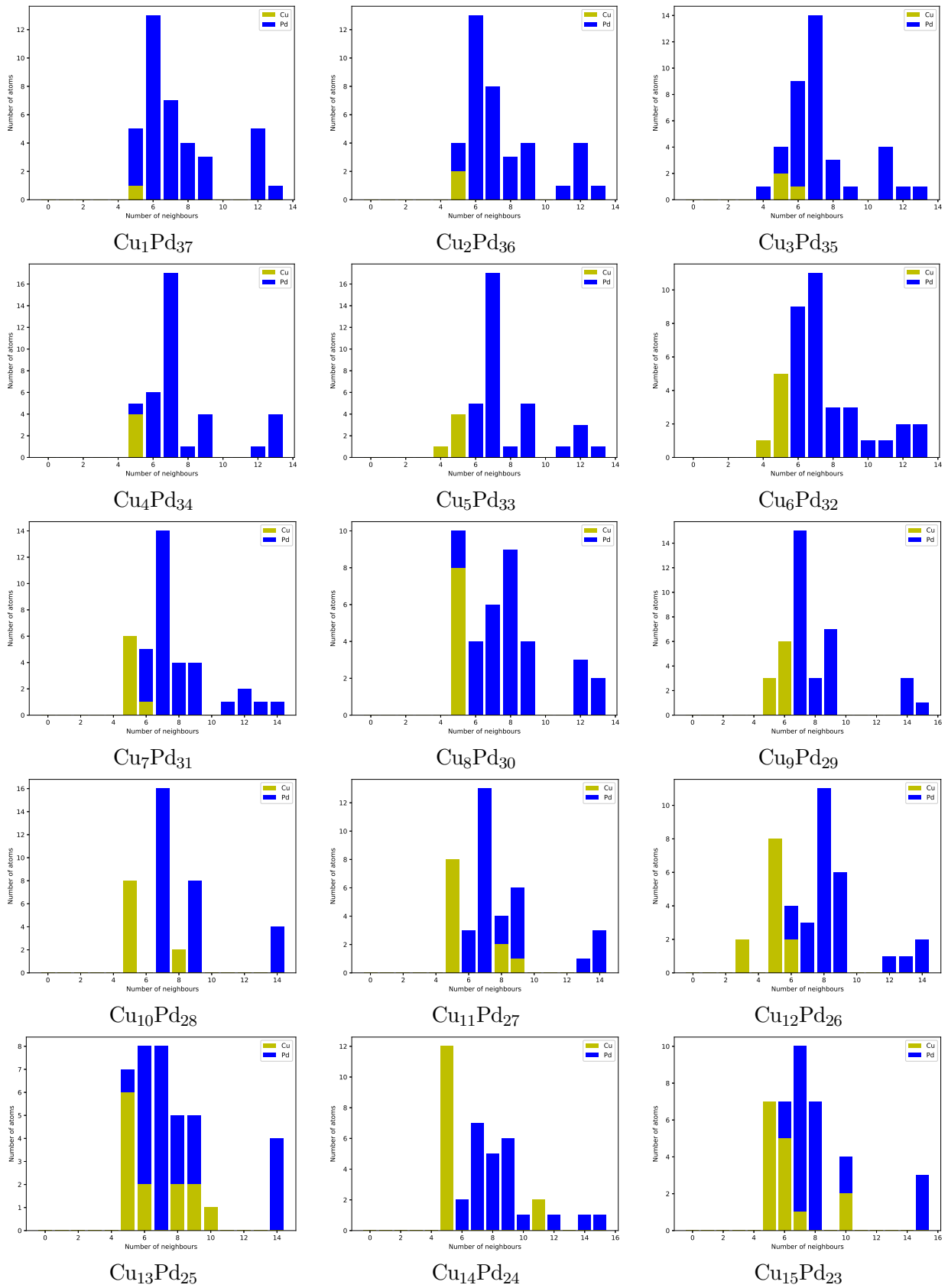
Figure 16: The nearest neighbour analyses calculated for GM clusters of all compositions found in a global optimisation run with GPS M.

Figure 17: The nearest neighbour analyses calculated for GM clusters of all compositions found in a global optimisation run with GPS M *cont'd*.

$Cu_{31}Pd_7$

$Cu_{32}Pd_6$

$Cu_{33}Pd_5$

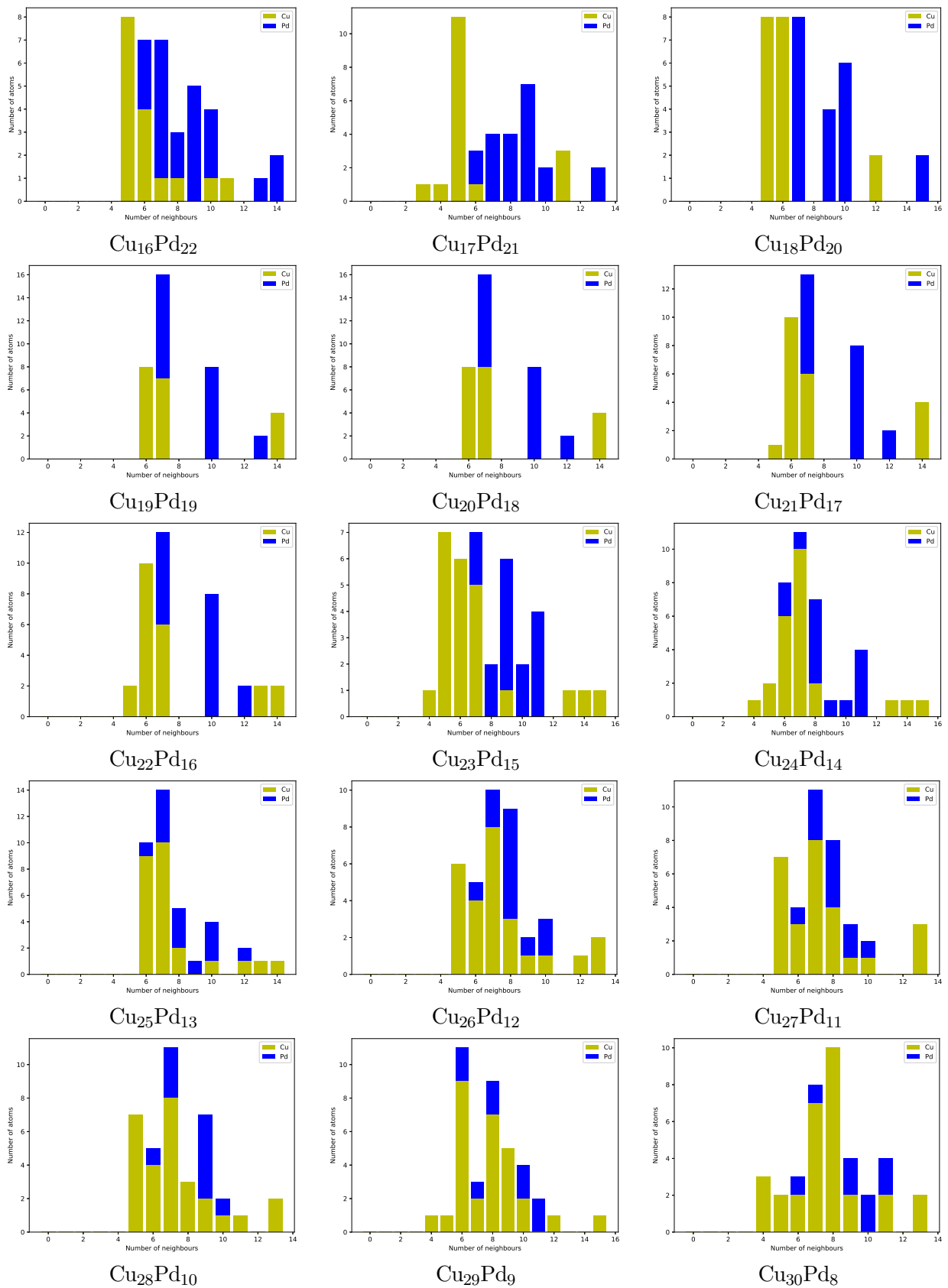$Cu_{34}Pd_4$

$Cu_{35}Pd_3$

$Cu_{36}Pd_2$

$Cu_{37}Pd_1$

Figure 18: The nearest neighbour analyses calculated for GM clusters of all compositions found in a global optimisation run with GPS M *cont'd.*
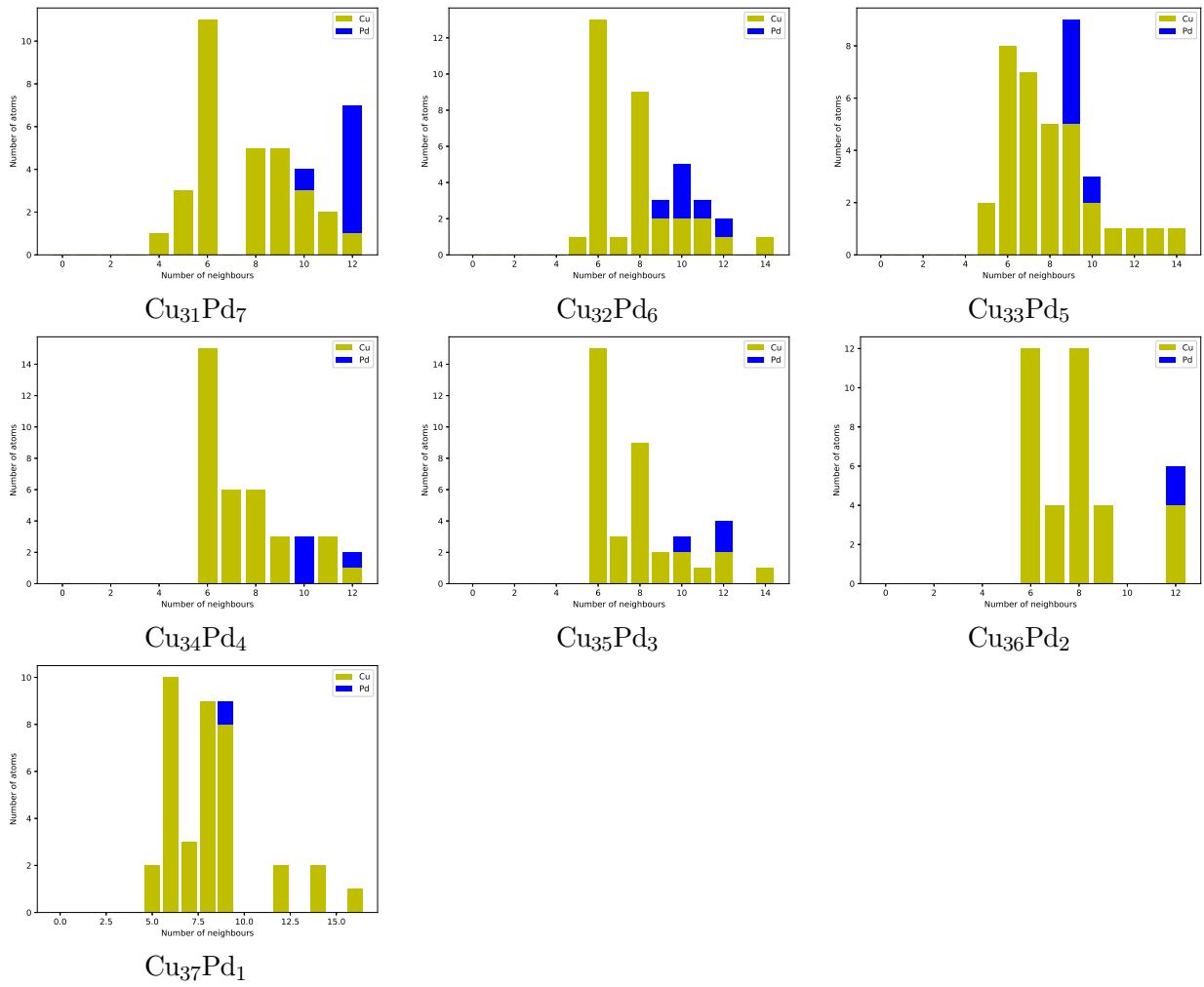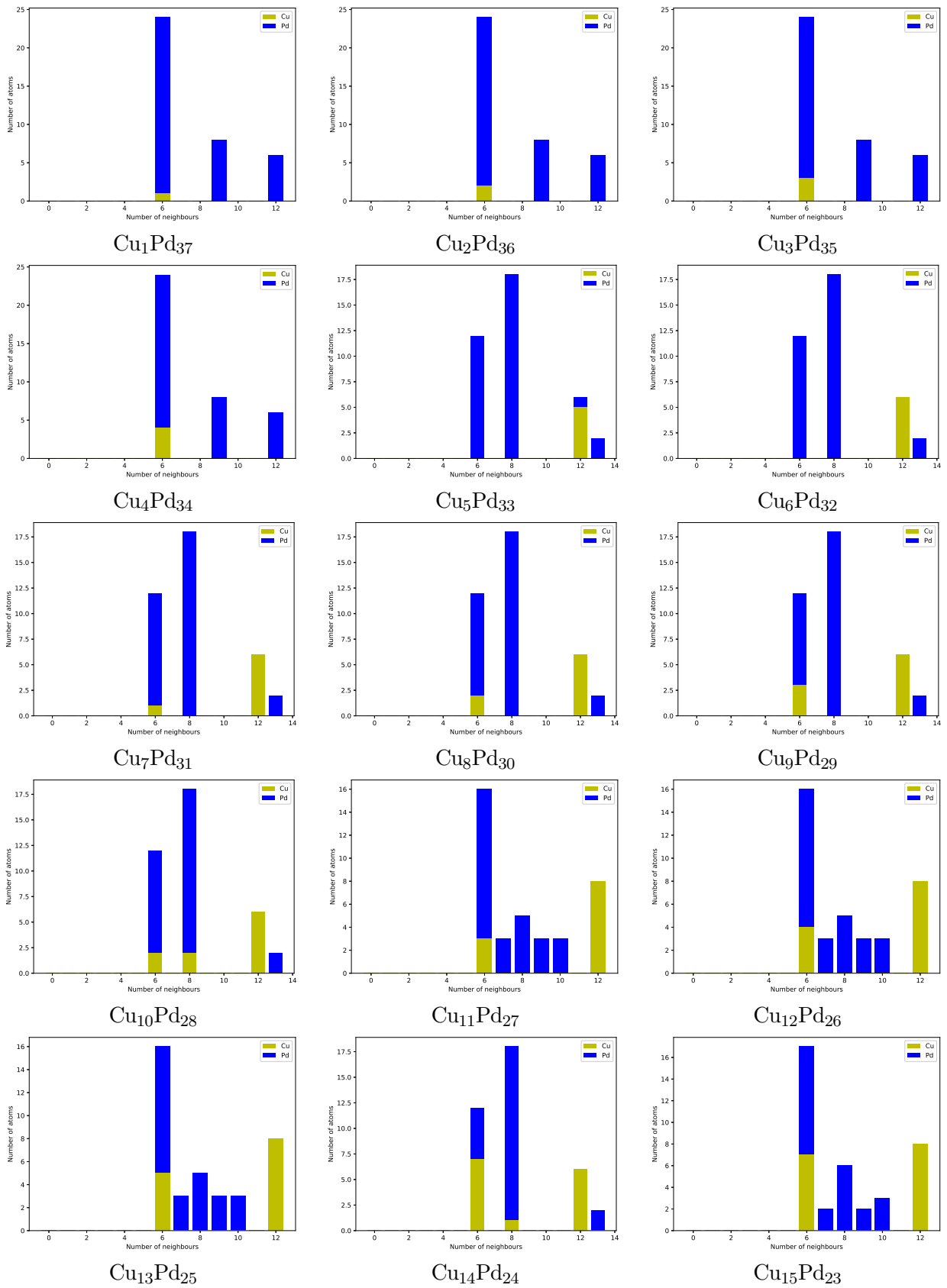
Figure 19: The nearest neighbour analyses calculated for GM clusters of all compositions found in a global optimisation run with GPS P/N.
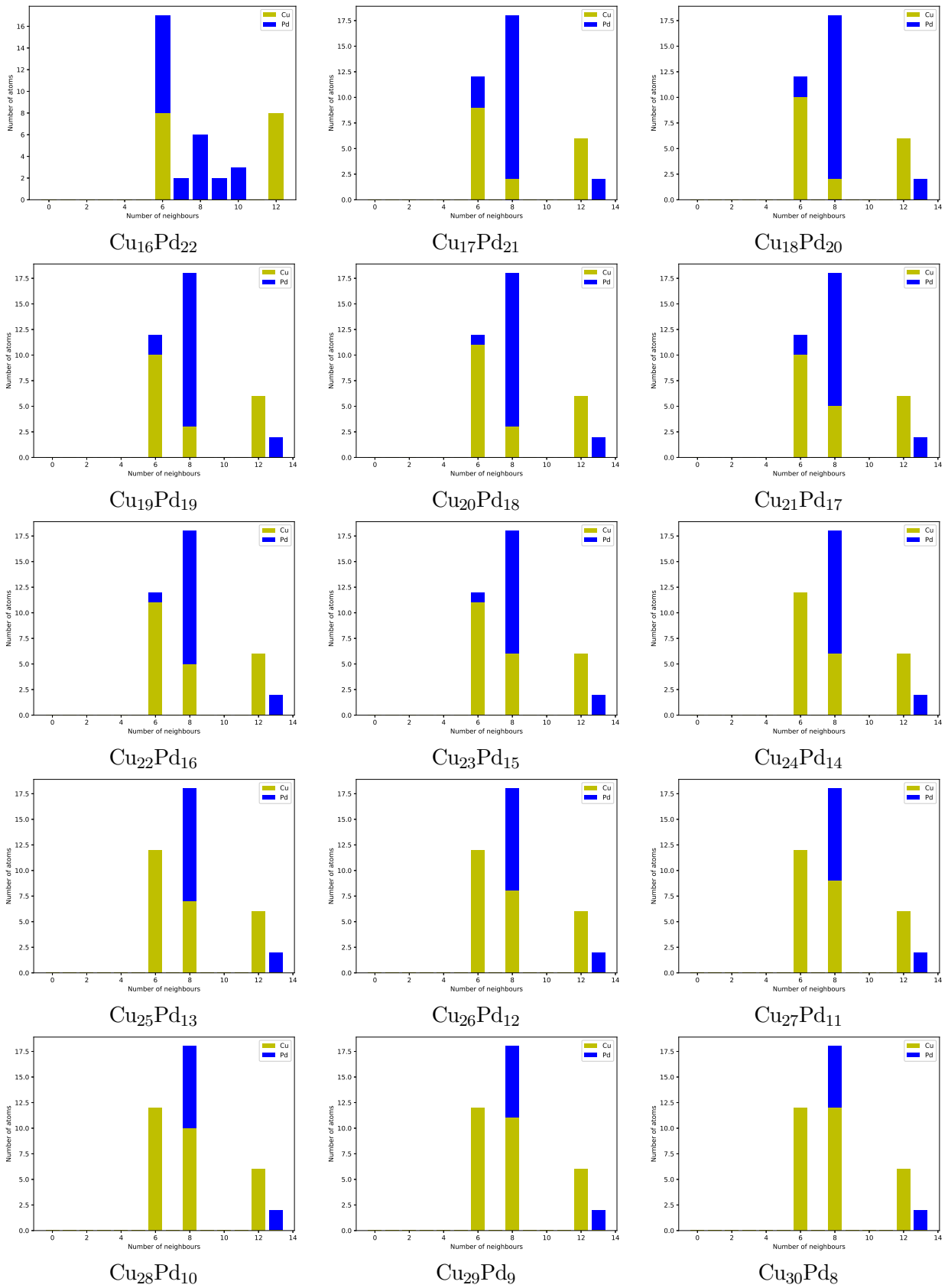
Figure 20: The nearest neighbour analyses calculated for GM clusters of all compositions found in a global optimisation run with GPS P/N *cont'd*.

$Cu_{31}Pd_7$

$Cu_{32}Pd_6$

$Cu_{33}Pd_5$

$Cu_{34}Pd_4$

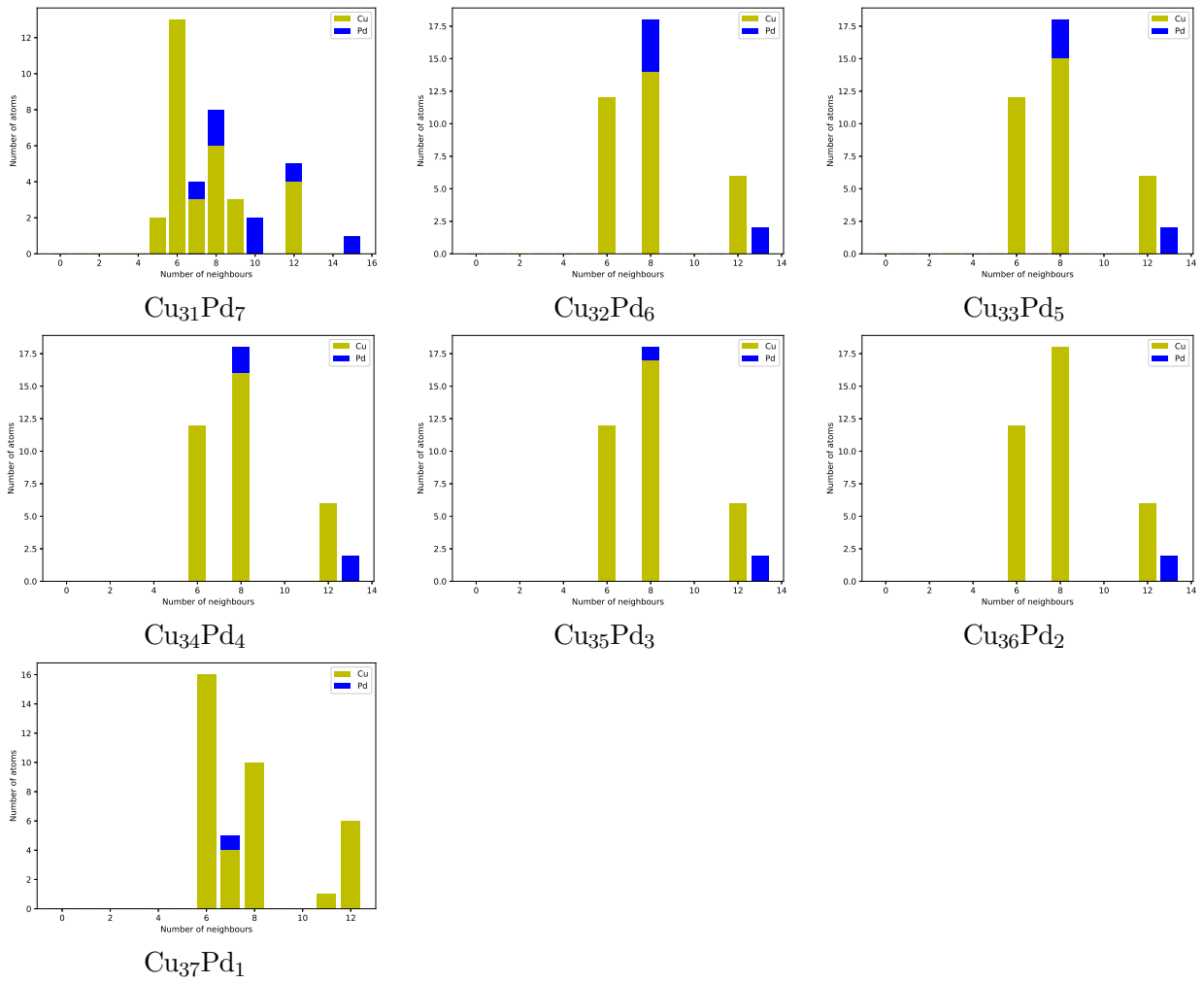$Cu_{35}Pd_3$

$Cu_{36}Pd_2$

$Cu_{37}Pd_1$

Figure 21: The nearest neighbour analyses calculated for GM clusters of all compositions found in a global optimisation run with GPS P/N *cont'd.*

Figure 22: The nearest neighbour analyses calculated for GM clusters of all compositions as found by DFT refinement of the GM clusters from the global optimisation runs of each GPS.

$Cu_{16}Pd_{22}$ $\quad$ $Cu_{17}Pd_{21}$ $\quad$ $Cu_{18}Pd_{20}$

$Cu_{19}Pd_{19}$ $\quad$ $Cu_{20}Pd_{18}$ $\quad$ $Cu_{21}Pd_{17}$

$Cu_{22}Pd_{16}$ $\quad$ $Cu_{23}Pd_{15}$ $\quad$ $Cu_{24}Pd_{14}$

$Cu_{25}Pd_{13}$ $\quad$ $Cu_{26}Pd_{12}$ $\quad$ $Cu_{27}Pd_{11}$

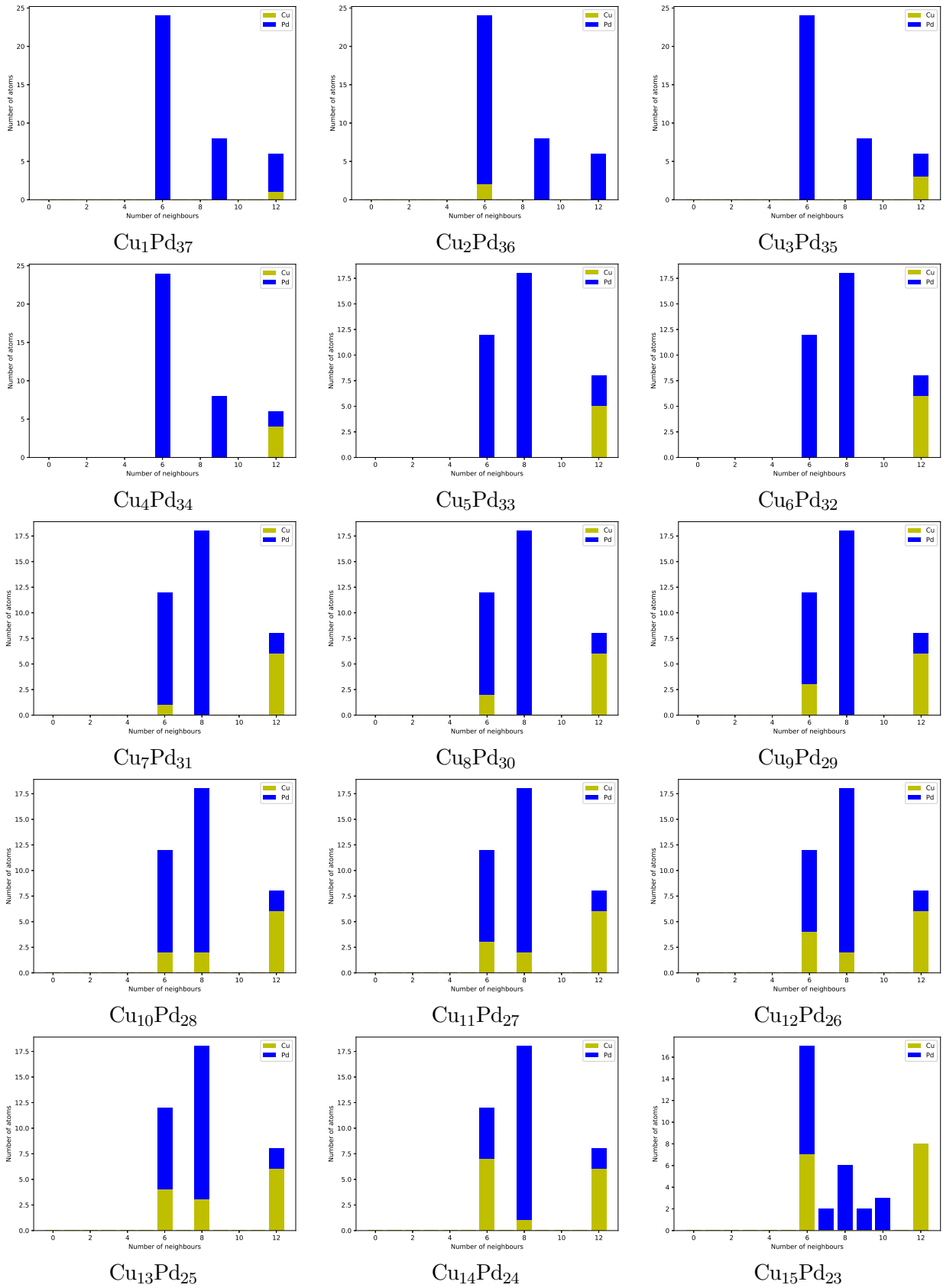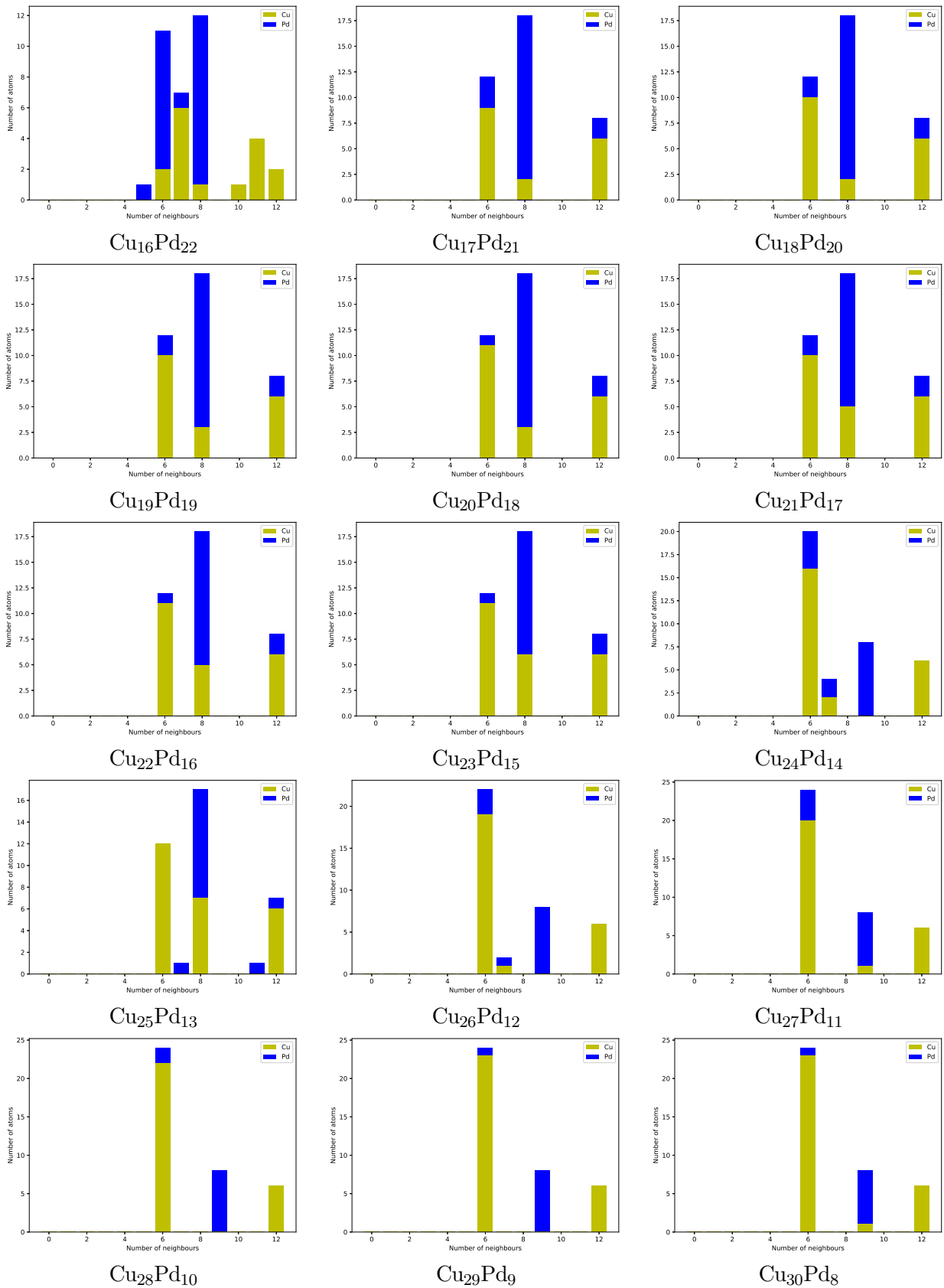$Cu_{28}Pd_{10}$ $\quad$ $Cu_{29}Pd_{9}$ $\quad$ $Cu_{30}Pd_{8}$

Figure 23: The nearest neighbour analyses calculated for GM clusters of all compositions as found by DFT refinement of the GM clusters from the global optimisation runs of each GPS *cont'd.*
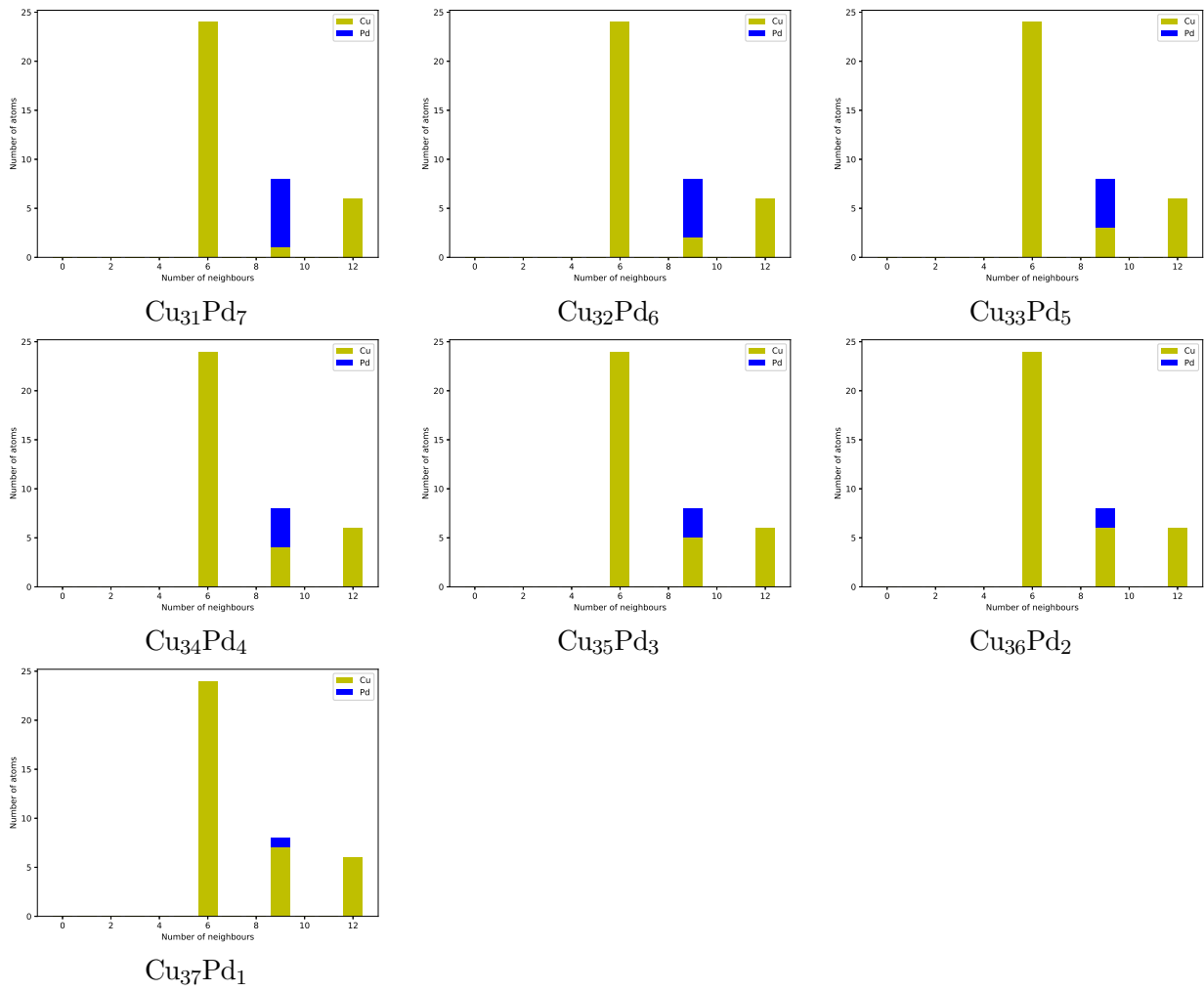
Figure 24: The nearest neighbour analyses calculated for GM clusters of all compositions as found by DFT refinement of the GM clusters from the global optimisation runs of each GPS *cont'd.*

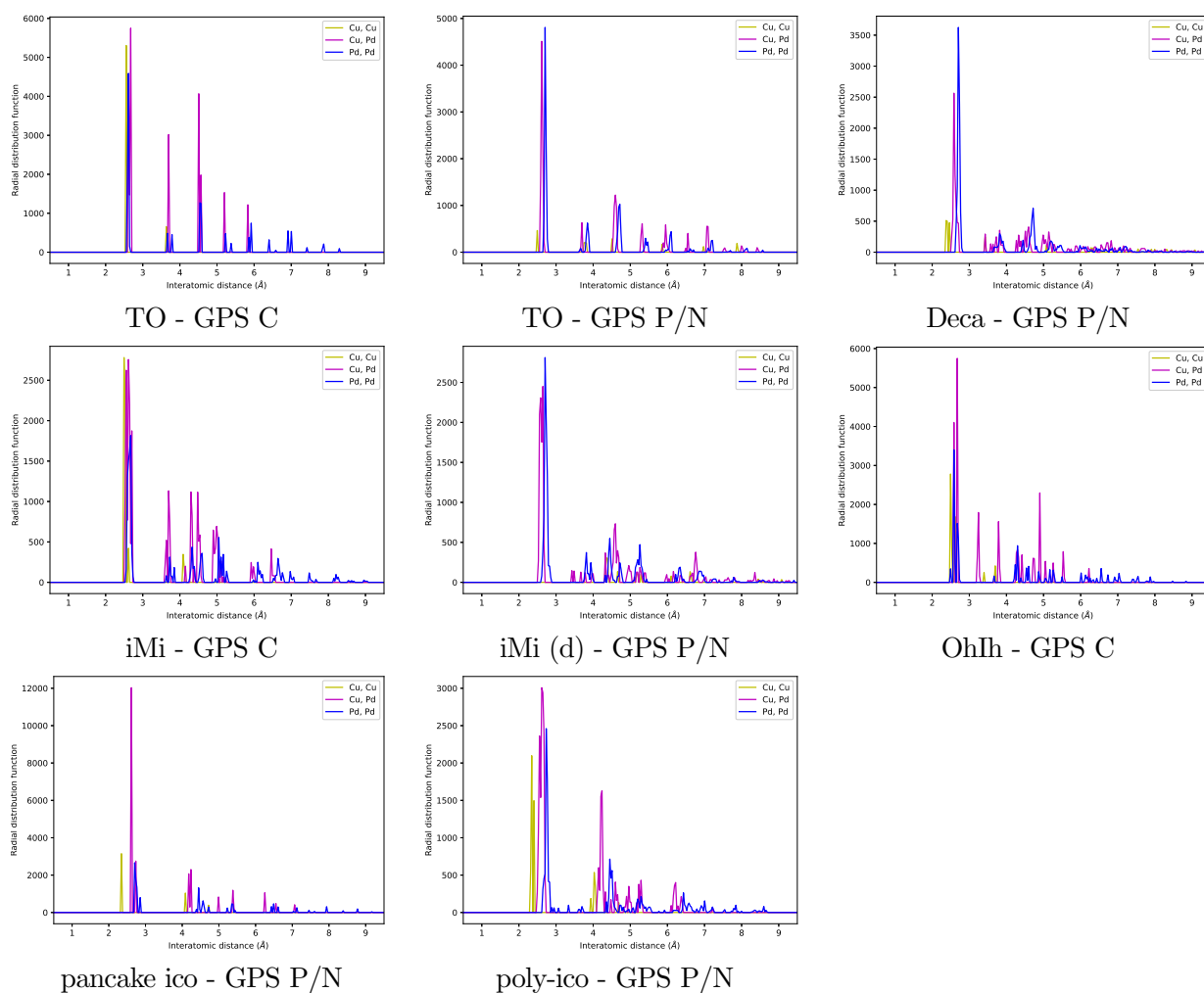# 3 Radial distribution functions of clusters from select compositions, as calculated with GPSs C and P/N.

TO - GPS C

TO - GPS P/N

Deca - GPS P/N

iMi - GPS C

iMi (d) - GPS P/N

OhIh - GPS C

pancake ico - GPS P/N

poly-ico - GPS P/N

Figure 25: The radial distribution functions calculated for selected Cu_6Pd_{32} clusters. Labels indicate the structural motif of the cluster and the GPS it was found with.
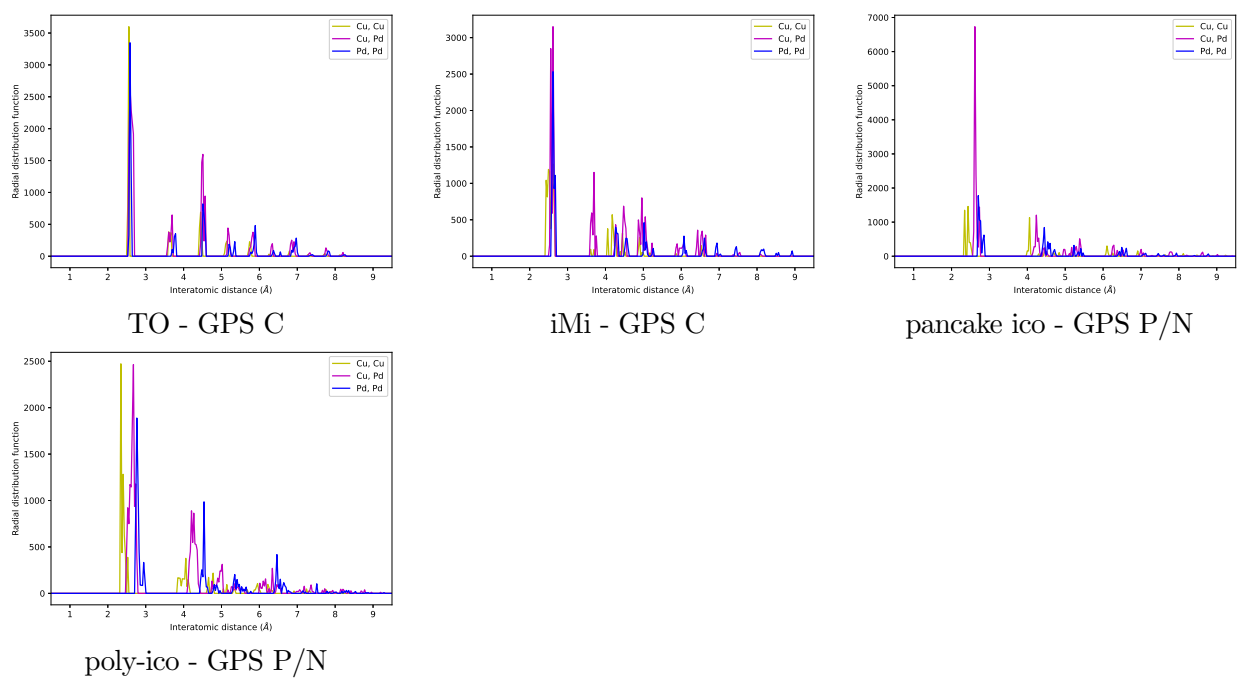
Figure 26: The radial distribution functions calculated for selected $Cu_{14}Pd_{24}$ clusters. Labels indicate the structural motif of the cluster and the GPS it was found with.
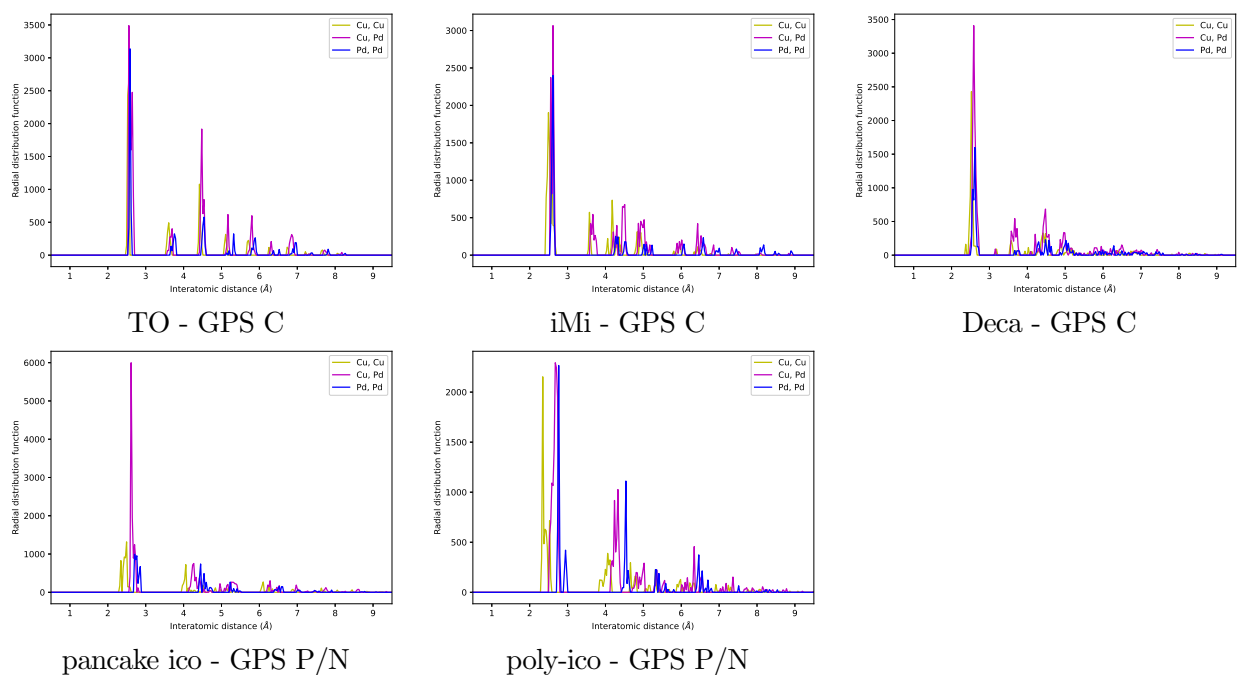

Figure 27: The radial distribution functions calculated for selected $Cu_{19}Pd_{19}$ clusters. Labels indicate the structural motif of the cluster and the GPS it was found with.

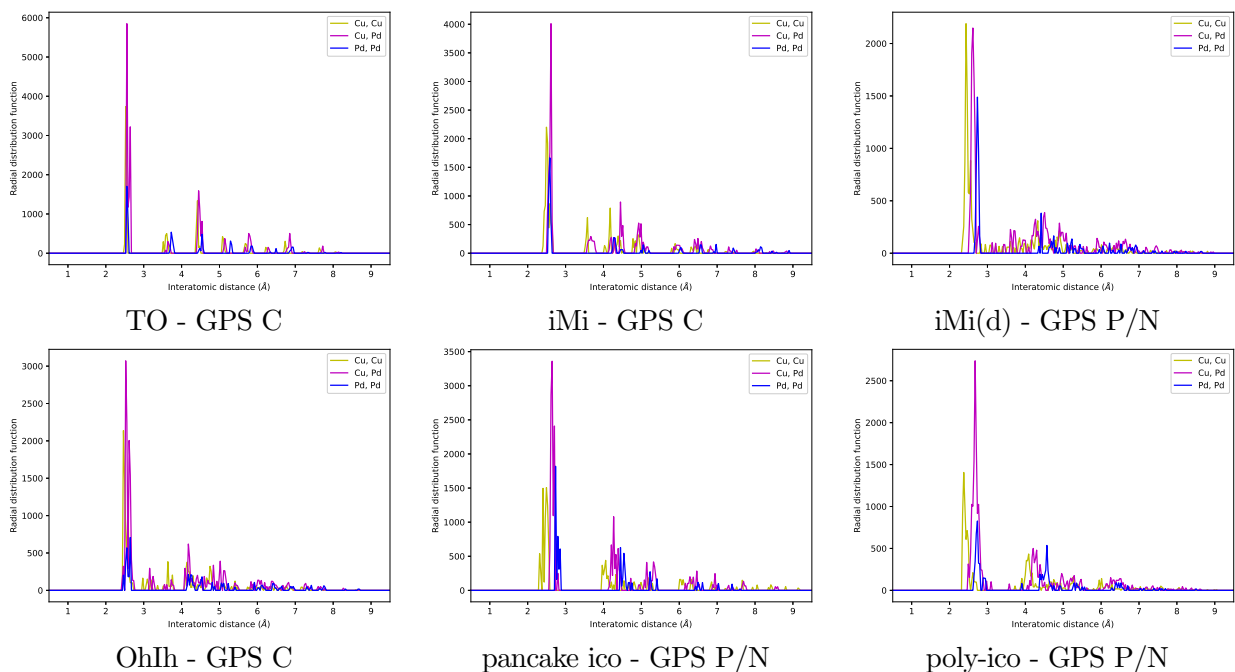TO - GPS C   iMi - GPS C   iMi(d) - GPS P/N

OhIh - GPS C   pancake ico - GPS P/N   poly-ico - GPS P/N

Figure 28: The radial distribution functions calculated for selected $Cu_{24}Pd_{14}$ clusters. Labels indicate the structural motif of the cluster and the GPS it was found with.

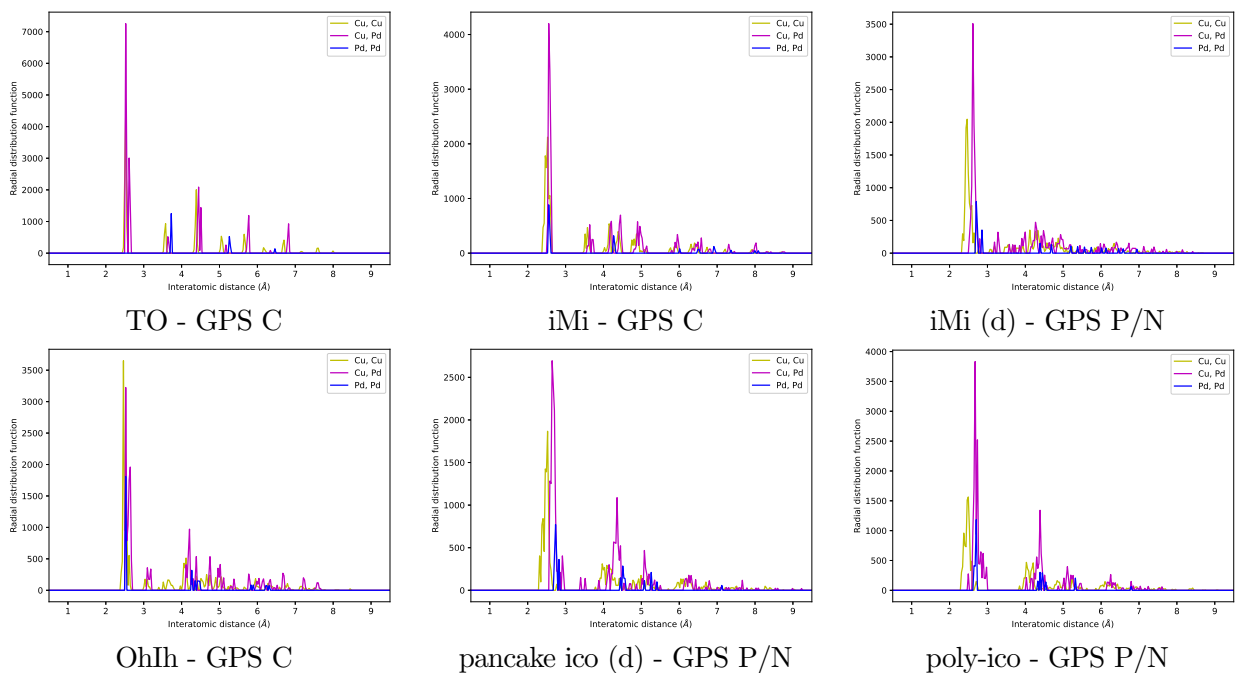TO - GPS C   iMi - GPS C   iMi (d) - GPS P/N

OhIh - GPS C   pancake ico (d) - GPS P/N   poly-ico - GPS P/N

Figure 29: The radial distribution functions calculated for selected $Cu_{32}Pd_6$ clusters. Labels indicate the structural motif of the cluster and the GPS it was found with.

4 Nearest neighbour analyses of clusters from select compositions, as calculated with GPSs C and P/N.
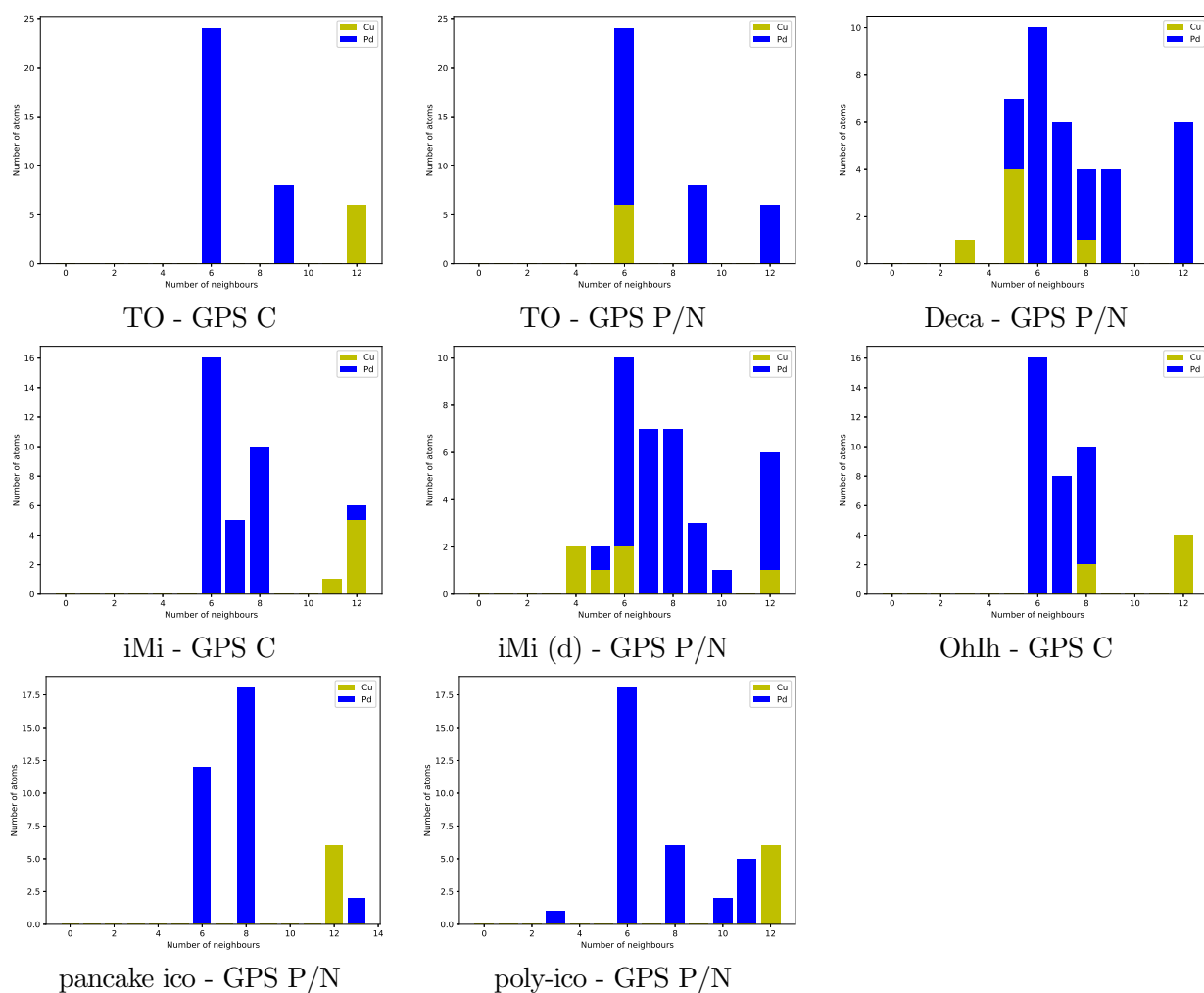

Figure 30: The nearest neighbour analyses for selected Cu_6Pd_{32} clusters. Labels indicate the structural motif of the cluster and the GPS it was found with.
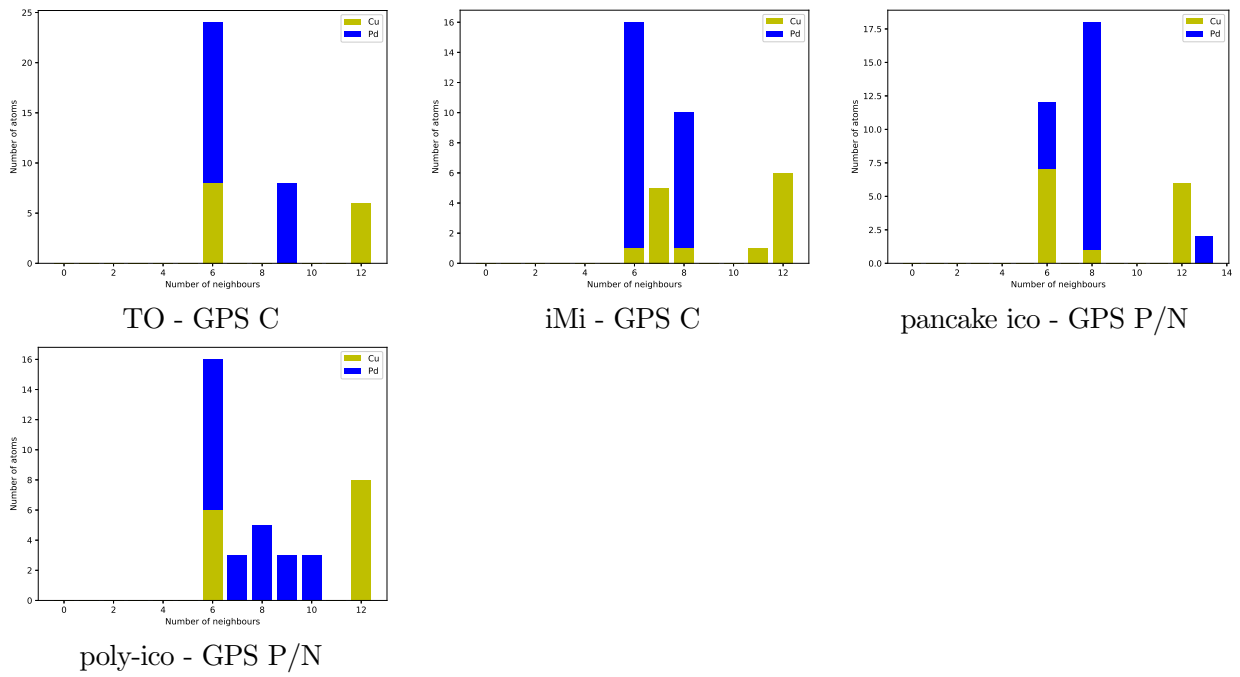
Figure 31: The nearest neighbour analyses for selected $Cu_{14}Pd_{24}$ clusters. Labels indicate the structural motif of the cluster and the GPS it was found with.
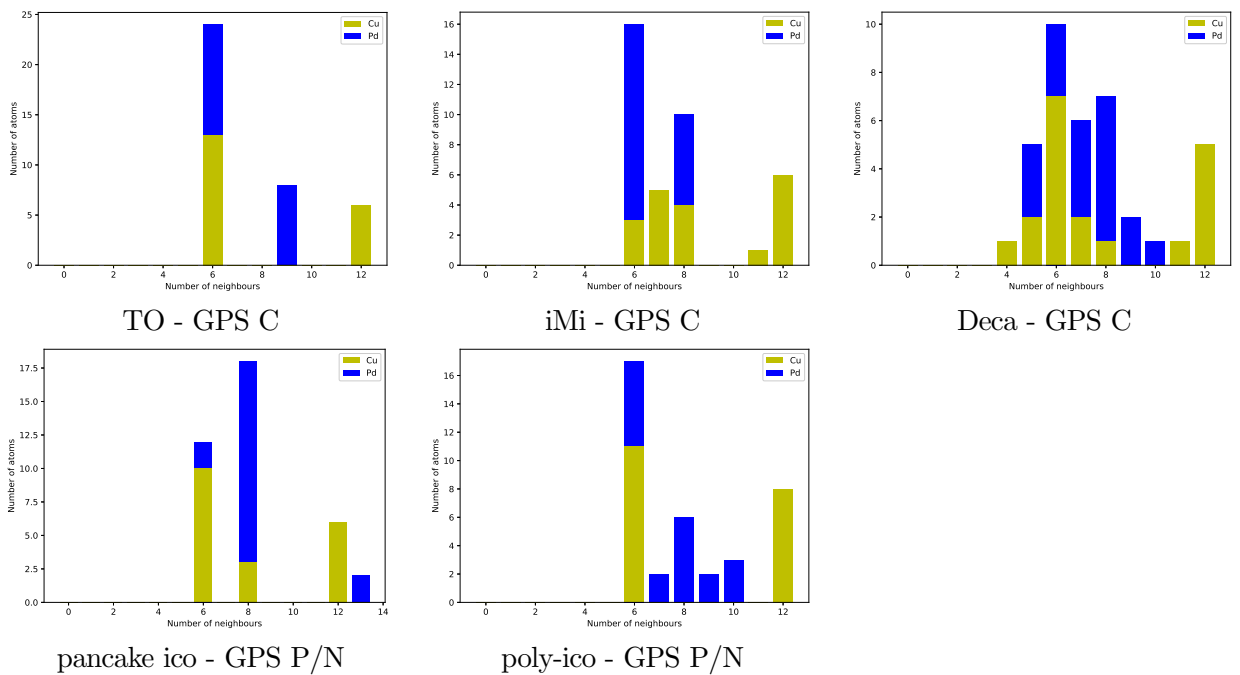

Figure 32: The nearest neighbour analyses for selected $Cu_{19}Pd_{19}$ clusters. Labels indicate the structural motif of the cluster and the GPS it was found with.
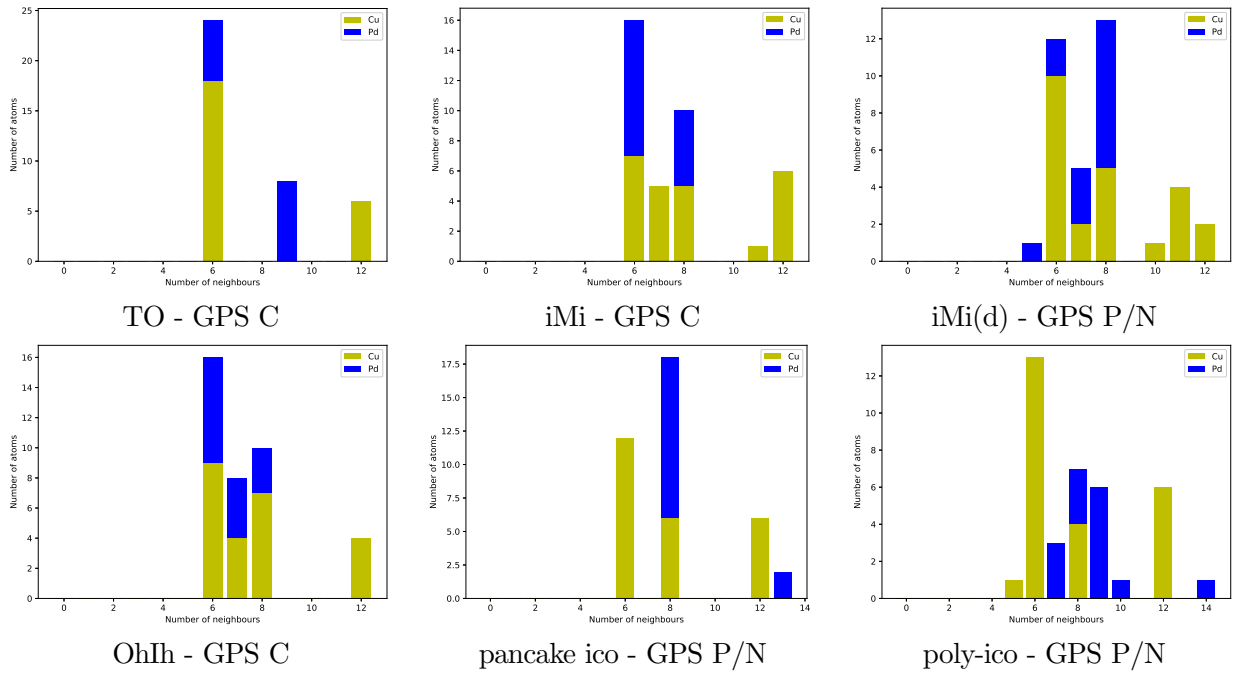
Figure 33: The nearest neighbour analyses for selected $Cu_{24}Pd_{14}$ clusters. Labels indicate the structural motif of the cluster and the GPS it was found with.
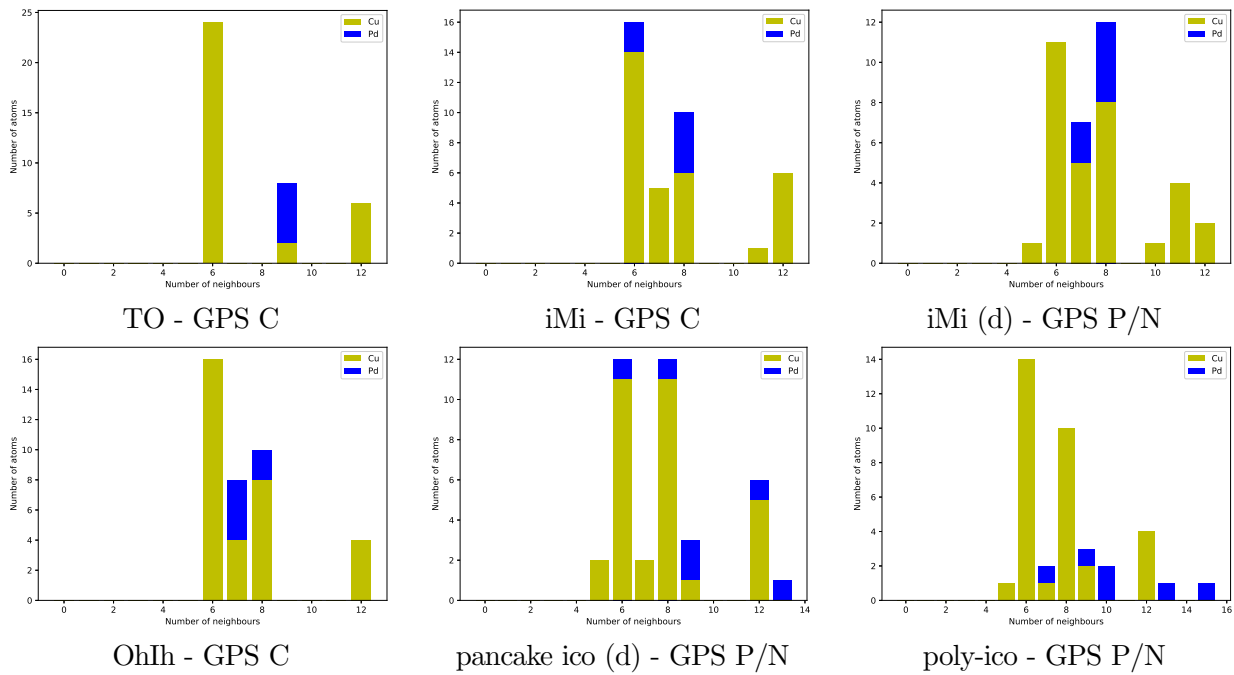

Figure 34: The nearest neighbour analyses for selected $Cu_{32}Pd_6$ clusters. Labels indicate the structural motif of the cluster and the GPS it was found with.